mathematics

MDPI

Article

Optimizing Retaining Walls through Reinforcement Learning Approaches and Metaheuristic Techniques

José Lemus-Romani [1], Diego Ossandón [2], Rocío Sepúlveda [2], Nicolás Carrasco-Astudillo [1], Victor Yepes [3] and José García [2,*]

[1] Pontificia Universidad Católica de Chile, Facultad de Ingeniería, Escuela de Construcción Civil, Santiago 7820436, Chile; jose.lemus@uc.cl (J.L.-R.)
[2] Pontificia Universidad Católica de Valparaíso, Facultad de Ingeniería, Escuela de Ingeniería de Construcción y Transporte, Valparaíso 2362807, Chile
[3] Universitat Politècnica de València, Institute of Concrete Science and Technology (ICITECH), 46022 València, Spain
* Correspondence: jose.garcia@pucv.cl

Abstract: The structural design of civil works is closely tied to empirical knowledge and the design professional's experience. Based on this, adequate designs are generated in terms of strength, operability, and durability. However, such designs can be optimized to reduce conditions associated with the structure's design and execution, such as costs, CO_2 emissions, and related earthworks. In this study, a new discretization technique based on reinforcement learning and transfer functions is developed. The application of metaheuristic techniques to the retaining wall problem is examined, defining two objective functions: cost and CO_2 emissions. An extensive comparison is made with various metaheuristics and brute force methods, where the results show that the S-shaped transfer functions consistently yield more robust outcomes.

Keywords: metaheuristics; concrete retaining walls

MSC: 90C27

Citation: Lemus-Romani, J.; Ossandón, D.; Sepúlveda, R.; Carrasco-Astudillo, N.; Yepes, V.; García, J. Optimizing Retaining Walls through Reinforcement Learning Approaches and Metaheuristic Techniques. *Mathematics* **2023**, *11*, 2104. https://doi.org/10.3390/math11092104

Academic Editor: Frank Werner

Received: 17 March 2023
Revised: 21 April 2023
Accepted: 23 April 2023
Published: 28 April 2023

1. Introduction

Today's society is experiencing a period of rapid growth and technological advancement that has accelerated exponentially over the years. This progression compels various industries to modernize, adapting to the evolving needs of consumers and the available resources and technologies. In this context, the construction industry has made significant strides in its design methods, gradually incorporating innovative techniques that pave the way for interdisciplinary approaches. These advancements ensure that civil work designs are optimized in terms of cost, material usage, associated carbon emissions, and other critical parameters [1].

In the realm of sustainable design, it is important to recognize that the construction industry is responsible for 33% of the energy produced globally and 30% of the total greenhouse gas emissions worldwide [2]. This significant environmental impact stems from the considerable carbon dioxide emissions associated with various elements in civil works [3]. These include the materials and machinery utilized throughout a project's life cycle from construction and maintenance to eventual demolition [4]. As a result, the need for more sustainable practices and a reduced ecological footprint in the construction industry has become increasingly evident.

Given the pressing climate emergency, numerous processes and industries have been compelled to adopt sustainable measures or update existing practices. Developing sustainable building approaches can help mitigate the environmental impacts caused by human activity [5]. This global environmental situation has urged the construction sector to adopt

and implement strategies to reduce or mitigate its ecological impact. Regarding carbon emissions, several studies have sought to minimize this parameter in various structures. For instance, ref. [6] employs a Finite Element Model (FEM) and a multi-objective genetic algorithm in the BIM modeling process to reduce a building's carbon emissions. Similarly, ref. [3] presents a comprehensive calculation of emissions involved in the life cycle of road construction, from material extraction to the end of its useful life, emphasizing the importance of earthworks and machinery efficiency. The study also highlights the relevance of material selection in optimizing emissions.

In [7], the researchers economically optimized footings using the MINLP (Mixed-Integer Non-Linear Programming) method. This study achieved a significant reduction of up to 63% in the total cost of the analyzed foundations. Additionally, various examples in the literature demonstrate the application of artificial intelligence algorithms within the construction industry. These include the use of computer vision for detecting cracks and defects in buildings [8], pavements [9], and bridges [10], as well as object detection on construction sites [11] and masonry segmentation [12].

In the domain of retaining walls, similar research efforts have been undertaken. For instance, ref. [13] presents a hybrid metaheuristic optimization method called h-BOASOS that minimizes the weight and cost of cantilever retaining walls. This approach combines the butterfly optimization algorithm (BOA) and symbiosis organism search (SOS) algorithm, outperforming other algorithms in benchmark tests, real-world engineering design problems, and cantilever retaining wall problems of various heights. In [14], the authors propose a hybrid k-means cuckoo search algorithm, merging the cuckoo search metaheuristic for continuous space optimization with the unsupervised k-means learning technique for discretizing solutions. The algorithm employs a random operator to assess the k-means operator's contribution and is benchmarked against a harmony search variant. The results reveal that incorporating the k-means operator significantly improves the solution quality, and the hybrid algorithm surpasses the harmony search approach. Finally, ref. [15] applies the shuffled shepherd optimization algorithm (SSOA) to optimize reinforced concrete cantilever retaining wall structures under static and seismic loading conditions. The optimization seeks to minimize the cost while adhering to stability and strength constraints based on ACI 318-05 requirements. Comparing SSOA results with other meta-heuristics highlights the algorithm's accuracy and convergence rate efficiency.

The numerous studies mentioned above highlight the ongoing efforts to optimize the design of various civil engineering elements and emphasize the importance of interdisciplinary collaboration in updating the industry. This article outlines the development process for optimizing retaining walls. Firstly, it explains the structural calculations and considerations required for designing the retaining wall. The second section discusses optimization techniques, their functionality, and their application to the problem.

Following this, the associated calculation model is parameterized to comply with the design standards, identifying crucial design aspects that can serve as variables in the optimization process. Subsequently, objective functions for each aspect are defined: one equation determines the economic cost, while another calculates carbon dioxide emissions, both applied to the retaining wall model.

Finally, a new algorithm that solves discrete problems using metaheuristics that naturally operate in continuous search spaces is proposed. Specifically, metaheuristic techniques such as the Sine Cosine Algorithm (SCA), Whale Optimization Algorithm (WOA), and Gray Wolf Optimization (GWO) are employed and integrated with SARSA and QL reinforcement learning techniques to address the discrete retaining wall problem and assess their performance and computational times. Statistical tests are used to compare the significance of the results obtained.

Extensive experiments were conducted to compare the implemented techniques, yielding notably robust and favorable results for static methods using S-shaped transfer functions. These results were obtained from 31 independent runs and their significance was validated through the Wilcoxon–Mann–Whitney [16] statistical test. The remainder of the paper is organized as follows: Section 2 outlines the retaining wall problem's modeling, while Section 3 introduces the optimization techniques. Section 4 presents the experimental findings, and Section 5 concludes the paper with discussions and final observations.

2. Concrete Retaining Walls

The present section lists the most critical design parameters considered. However, before delving into them, it is necessary to know the initial condition of the problem under consideration. At this point, it should be noted that the model considers the design of a cantilever-type wall with a structural backfill that has known resistance parameters and no overload. Furthermore, in geometrical terms, the model analyzes one linear wall meter as the problem's initial condition. Finally, the selection of the number and diameter of bars that meet the design requirements will be determined using the same. Having said that, the main calculation bases are detailed below.

Calculation of applicants: The design proposes that the structural fill exerts two types of thrust on the wall. The first type corresponds to the thrust of the soil under static conditions, while the second type corresponds to the thrust generated by the soil under pseudo-static (seismic) conditions [17]. These concepts are represented by Equations (1) and (2).

$$qe = c \cdot \gamma \cdot hz \cdot b \tag{1}$$

where:
qe = Static thrust exerted by the fill [T/m]
γ = Existing soil density [T/m^3].
z = Height of the wall [m].
c = Static thrust coefficient.
b = Wall width, corresponding to 1 [m].

$$qs = cs \cdot \gamma \cdot hz \cdot b \tag{2}$$

where:
qs = Seismic thrust exerted by the backfill [T/m].
γ = Existing soil density [T/m^3].
hz = Height of wall [m].
cs = Seismic thrust coefficient.
b = Wall width, corresponding to 1 [m].

Calculation of the requesting moment at point A: The design outlines the calculation of forces at point A, defined as the most unfavorable point on the wall in terms of stress caused by the soil thrust. This condition is represented through Equation (3) and Figure 1.

$$MsA = M_{active} + M_{seismic} \tag{3}$$

where:
MsA = Moment calculated at point A [T · m].
M_{active} = Static moment generated by the ground at point A [T · m].
$M_{seismic}$ = Seismic moment generated by the ground at point A [T · m].

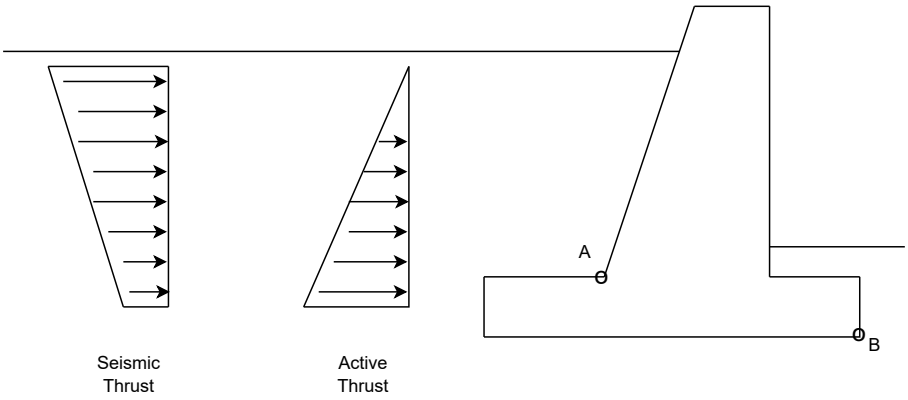

Figure 1. Stress distribution and location of point A in the retaining wall.

Quantification of the design requesting forces: Once the applied moment has been determined, the moment generated by the wall's self-weight at point A must be calculated. Finally, the applied moment is defined as the sum of the previously computed moments, which are then added to obtain the design moment and axial load, as illustrated in Equations (4)–(7).

$$M_{pp} = d1 \cdot N1 + d2 \cdot N2 \tag{4}$$

where:
M_{pp} = Moment generated by the self-weight at point A [T · m].
$d1$ = Distance from the centroid of the **prismatic** section of the wall to point A [m].
$N1$ = Eigenweight of the **prismatic** section of the wall [T].
$d2$ = Distance from the centroid of the **triangular** section of the wall to point A [m].
$N2$ = Eigenweight of the **triangular** section of the wall [T].

$$MA = MsA + M_{pp} \tag{5}$$

where:
MA = Total moment at point A [T · m].
MsA = Moment calculated at point A [T · m].
M_{pp} = Moment generated by self-weight at point A [T · m].

$$M_{eu} = MA \cdot \gamma f \tag{6}$$

where:
Meu = Design moment [T · m].
MA = Total moment at point A [T · m].
γf = Moment majorization factor.

$$N_u = N_t \cdot \gamma f \tag{7}$$

where:
Nu = Design axial load [T].
Nt = Own weight of the wall [T].
γf = Moment magnification factor.

Steel amount for stirrups: For the calculation of the reinforcement required in the wall stirrups, the dimensionless method is applied, defined through Equations (8)–(11).

$$\mu = \frac{M_{eu}}{\phi \cdot \beta \cdot f'c \cdot b \cdot d} \tag{8}$$

where:
μ = Dimensionless calculation factor.
M_{eu} = Design moment [T · m].

ϕ = Reduction factor for flexocompression equal to 0.83.
β = Reduction of the characteristic strength of concrete equal to 0.85.
$f'c$ = Characteristic resistance of concrete to compression [T/m^2].
b = Width of the wall, corresponding to 1 [m].
d = Width of the base of the wall without covering [m].

$$\nu = \frac{N_u}{\phi \cdot \beta \cdot f'c \cdot b \cdot d} \tag{9}$$

where:
ν = Dimensionless shear factor in the structure.
N_u = Design axial load [T].
ϕ = Reduction factor for flexocompression equal to 0.83.
β = Reduction of the characteristic strength of concrete equal to 0.85.
$f'c$ = Characteristic resistance of concrete to compression [T/m^2].
b = Width of the wall, corresponding to 1 [m].
d = Width of the base of the wall without covering [m].

$$w = 1 - \sqrt{1 - 2 \cdot \mu} - \nu \tag{10}$$

where:
w = Calculation ratio for the steel area.
μ = Calculation dimensionless factor.
ν = Dimensionless shear factor in the structure.

$$A = \frac{w \cdot \beta \cdot f'c \cdot b \cdot d}{f_y} \tag{11}$$

where:
A = Required steel area [cm^2].
w = Calculation ratio for steel area .
β = Reduction of the characteristic strength of the concrete equal to 0.85.
$f'c$ = Characteristic resistance of concrete to compression [T $*$ m^2].
b = Width of the wall, corresponding to 1 [m].
d = Width of the base of the wall without covering [m].
f_y = Steel creep [T/cm^2].

Verification of overturning resistance: For the overturning resistance verification, two central moments must be determined. The first one corresponds to the resistant moment exerted by the wall's self-weight, the foundation, and the soil on the bottom (Figure 2 and Equation (12)) up to the outermost point of the wall (the lower end of the foundation), defined as point B. Similarly, the moment generated by the active and seismic thrusts up to that point must be determined (Equation (13)). With this information, it is possible to calculate the overturning safety factor using Equations (14) and (15).

$$Mr = Ns \cdot x1 + Nm \cdot x2 + N1 \cdot x3 + Nf \cdot x4 \tag{12}$$

where:
M_r = Overturning resisting moment [T · m].
Ns = Self-weight of soil on bottom [T].
$x1$ = Distance from the centroid of Ns to point B [m].
Nm = Dead weight of the wall wedge and the soil above it [T].
$x2$ = Distance from the centroid of Nm to point B [m].
$N1$ = Self weight of the prismatic section of the wall [T].
$x3$ = Distance from the centroid of N1 to point B [m].
Nf = Self weight of the wall foundation [T].

$x4$ = Distance from the centroid of Nf to point B [m].

$$MsB = M_{active}B + M_{seismic}B \tag{13}$$

where:
MSB = Moment calculated at point B [T · m].
$M_{active}B$ = Static moment generated by the soil at point B [T · m].
$M_{seismic}B$ = Seismic moment generated by the soil at point B [T · m].

$$FSSV = \frac{Mr}{MsB} \tag{14}$$

where:
$FSSV$ = Overturning seismic safety factor.
Mr = Moment resisting overturning [T · m].
MsB = Moment calculated at point B [T · m].

$$FSEV = \frac{Mr}{M_{active}B} \tag{15}$$

where:
$FSEV$ = Rollover static safety factor. Mr = Moment resisting overturning [T · m].
MsB = Moment calculated at point B [T · m].

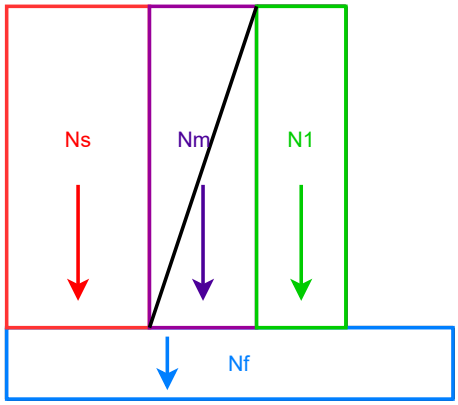

Figure 2. Resisting forces acting on the retaining wall.

Slip resistance verification: The procedure for the slip resistance verification follows the same principle as the rollover verification; that is, the applicant and resistant forces must be determined through Equations (16)–(19).

$$Fsol = (qe + qs) \cdot b \tag{16}$$

where:
$Fsol$ = Slip requesting force [T].
qe = Static thrust exerted by the filler [T/m].
qs = Seismic thrust exerted by the backfill [T/m].
b = Width of the wall, corresponding to 1 [m].

$$Fres = (Ns + Nm + N1 + Nf) \cdot \mu \tag{17}$$

where:
$Fres$ = Slip-resistant forces [T].
Ns = Self-weight of the soil on the bottom [T].
Nm = Self-weight of the wall wedge and the soil above it [T].
$N1$ = Self-weight of the prismatic section of the wall [T].

Nf = Self-weight of the wall foundation [T].
μ = Coefficient of friction between the foundation and the soil.

$$FSSD = \frac{Fres}{Fsol} \tag{18}$$

where:
$FSSD$ = Seismic slip safety factor.
$Fres$ = Slip-resistant forces [T].
$Fsol$ = Slip-requesting force [T].

$$FSED = \frac{Fres}{qe} \tag{19}$$

where:
$FSSD$ = Seismic slip safety factor.
$Fres$ = Slip-resistant forces [T].
qe = Static thrust exerted by the filler [T].

Verification of allowable stress: Within the verification section, it is necessary to check that the stresses transmitted to the soil (maximum and minimum) do not exceed the allowable stress given by the previous geotechnical study. The verification is carried out by means of Equation (20).

$$\sigma = \frac{Ns + Nm + N1 + Nf}{L \cdot b} \pm \frac{MsB - Ns \cdot x1 + Nm \cdot x2 + N1 \cdot x3}{\frac{b \cdot L^2}{6}} \tag{20}$$

where:
σ = Stress transmitted to the foundation soil [T/m^2].
Ns = Self-weight of the soil on the bottom [T].
$x1$ = Distance from the centroid of Ns to point B [m].
Nm = Self-weight of the wall wedge and the soil above it [T].
$x2$ = Distance from the centroid of Nm to point B [m].
$N1$ = Self-weight of the prismatic section of the wall [T].
$x3$ = Distance from the centroid of N1 to point B [m].
Nf = Self-weight of the wall foundation [T].
L = Total length of the foundation [m].
b = Width of the wall, corresponding to 1 [m].
MsB = Moment calculated at point B [T · m].

Verification of percentage of support: Since the stress transmitted to the soil may adopt negative values, it must be checked that the foundation does not tend to lift out of the soil. Once the percentage of support has been defined, it is checked that the stress generated by the weight of the system does not exceed the admissible soil stress, with Equations (21)–(24).

$$e = \frac{MsB - Ns \cdot x1 + Nm \cdot x2 + N1 \cdot x3}{Ns + Nm + N1 + Nf} \tag{21}$$

where:
e = Eccentricity of forces [m].
Ns = Self-weight of the soil on the bottom [T].
$x1$ = Distance from the centroid of Ns to point B [m].
Nm = Self-weight of the wall wedge and the soil above it [T].
$x2$ = Distance from the centroid of Nm to point B [m].
$N1$ = Self-weight of the prismatic section of the wall [T].
$x3$ = Distance from the centroid of N1 to point B [m].

Nf = Self-weight of the wall foundation [T].
MsB = Moment calculated at point B [T · m].

$$g = 3 \cdot (\frac{L}{2} - e) \tag{22}$$

where:
g = Section of the foundation supported on the ground [m].
L = Total length of the foundation [m].
e = Eccentricity of forces [m].

$$\sigma effective = \frac{2 \cdot (Ns + Nm + N1 + Nf)}{b \cdot g} \tag{23}$$

where:
$\sigma_effective$ = Effective stress applied to the foundation soil.
Ns = Self-weight of the soil on the bottom [T].
Nm = Self-weight of the wall wedge and the soil above it [T].
$N1$ = Self-weight of the prismatic section of the wall [T].
Nf = Self-weight of the wall foundation [T].
b = Width of the wall, which corresponds to 1 [m].
g = Section of the foundation supported on the ground [m].

$$\%ofsupport = \frac{g}{L} \tag{24}$$

where:
g = Section of the foundation supported on the ground [m].
L = Total length of the foundation [m].

Reinforcing reinforcement for foundation under structural backfill: The uplift effect generated by the negative tension in the soffit area can generate additional tensile stresses in the foundation, so a reinforcement must be sized in the footing located in the soffit area of the wall. For this purpose, the design moment is determined from the forces involved (Figure 3) and then the dimensionless method is applied (Equation (25)).

$$Mdesign = 1.4 \cdot (Msr + Mf - Msf) \tag{25}$$

where:
$Mdesign$ = Design moment of reinforcement reinforcement [T · m].
Msr = Moment generated by backfill soil measured at design point [T · m].
Mf = Moment generated by the foundation measured at the design point [T · m].
Msf = Moment generated by the foundation soil measured at design point [T · m].

Foundation armor: In addition to the reinforcement calculated above, a reinforcement for the foundation, both longitudinal and transverse, must be dimensioned. This is carried out by means of Equations (26) and (27).

$$Mdl = (\frac{Bdt - Bm}{2} \cdot b) \cdot (\frac{1.4 \cdot Pp}{L \cdot b}) \cdot (\frac{Bdt - Bm}{4}) \tag{26}$$

where:
Mdl = Design moment of longitudinal reinforcement [T · m].
Bdt = Maximum foundation flight [m].
Bm = Width of the wall base [m].
Pp = Self-weight of the wall [T].
L = Total length of foundation [m].
b = width of the wall, corresponding to 1 [m].

$$Mdt = \frac{1.4 \cdot Pp \cdot b^2}{2 \cdot 1[m]} \tag{27}$$

where:
Mdt = Design moment of transverse reinforcement [T · m].
Pp = Self-weight of the wall [T].
b = Width of the wall, which corresponds to 1 [m].

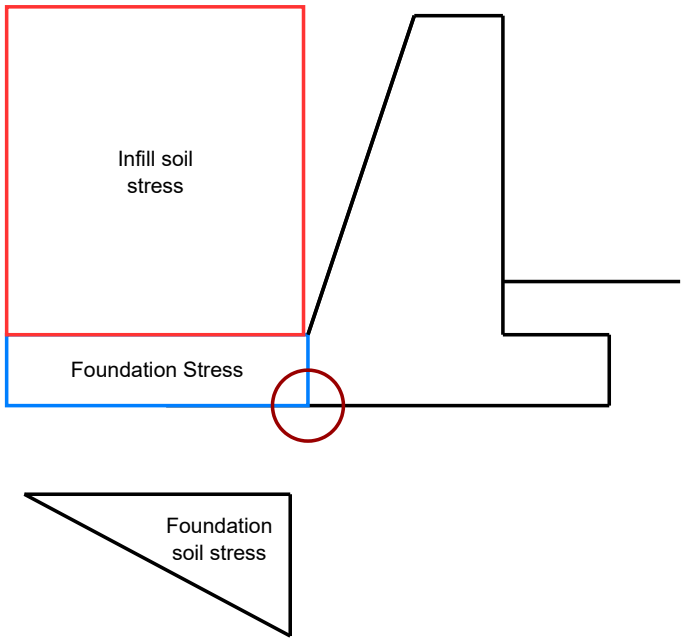

Figure 3. Stresses involved in structural reinforcement design.

Calculation of the steel area for the foundation: In the case of the reinforcement for the foundation, both longitudinal and transverse, the amount of steel required is determined with Equations (28) and (29).

$$T = \frac{Md}{0.9 \cdot d'} \tag{28}$$

where:
T = Design stress [T].
Md = Corresponding design moment (Mdl or Mdt) [T · m].
d' = Effective shoe height (height without cover) [m].

$$As = \frac{T}{0.9 \cdot Fy} \tag{29}$$

where:
As = Required steel area [cm^2].
T = Design stress generated by the design moment [T].
Fy = Yield stress of steel [T/cm^2].

Minimum armor: The amount of steel calculated above must be verified with respect to the corresponding minimum amount of steel, calculated through Equation (30).

$$emin = 0.0018 \cdot Ag \tag{30}$$

where:
$emin$ = Minimum amount of steel required [cm^2].
Ag = Longitudinal or cross-sectional area of the footing, as appropriate [cm^2].

Verification of concrete shear strength: Check if the designed concrete section has the required minimum shear strength through the Equations (31) and (32).

$$Vu = (\frac{Bdt - Bm}{2} - d) \cdot b \cdot \frac{1.4 \cdot Pp}{L \cdot b} \tag{31}$$

where:
Vu = Design cut request [T].
Bdt = Maximum foundation flight [m].
Bm = Width of wall base [m].
d = Thickness of the uncoated shoe [m].
Pp = Self-weight of the wall [T].
L = Total length of foundation [m].
b = Width of the wall, corresponding to 1 [m].

$$Vc = 0.53 \cdot \lambda \cdot \sqrt{f'c} \cdot b \cdot d \tag{32}$$

where:
Vc = Shear strength of concrete section [T].
λ = Concrete modification factor. For normal concrete, λ = 1.
$f'c$ = Characteristic compressive strength of concrete [T/m^2].
b = Width of the wall, which corresponds to 1 [m].
d = Thickness of the uncoated shoe [m].

2.1. Restrictions

The design problem must respond to specific constraints to be considered correct. These limitations, known as constraints, will be fundamental in determining whether the solution proposed in the optimization process is (or is not) valid. The following are the constraints identified.

$\boldsymbol{\mu}$**lim**: According to the initial conditions for the application of the dimensionless sizing method used to determine the amount of steel required, the relationship of Equation (33).

$$\boldsymbol{\mu = \mu lim} \tag{33}$$

where:
$\boldsymbol{\mu}$ = Dimensionless factor, calculated in Equation (8).
$\boldsymbol{\mu lim}$ = Calculation limit dimensionless factor, equal to 0.3047 for the case of analysis.

Slip safety factor: As with the overturning safety factor, a minimum value of slip safety factor must be met to avoid the occurrence of this type of failure. That said, the restriction is set forth in Equations (34) and (35).

$$\boldsymbol{FSED \geq 1.5} \tag{34}$$

where:
$\boldsymbol{FSED}$ = Static slip safety factor, calculated by Equation (19).

$$\boldsymbol{FSSD \geq 1.1} \tag{35}$$

where:
$\boldsymbol{FSSD}$ = Seismic slip safety factor, calculated by Equation (18).

Rollover safety factor: The design must meet minimum safety criteria [18], including the overturning safety factor, which avoids abrupt failures due to overturning when loads not foreseen in the initial design are applied. Under this criterion, the conditions are defined in Equations (36) and (37).

$$\boldsymbol{FSEV \geq 1.5} \tag{36}$$

where:
$\boldsymbol{FSEV}$ = Static rollover safety factor, calculated in Equation (15).

$$\boldsymbol{FSSV \geq 1.15 \cdot FSSD} \tag{37}$$

where:
$\boldsymbol{FSSV}$ = Seismic overturning factor of safety, calculated in Equation (14).
$\boldsymbol{FSSD}$ = Seismic safety factor to slip, calculated in Equation (19).

Allowable stress: As a minimum requirement, the stresses produced by the interaction between the foundation and the supporting soil must be lower than the allowable bearing capacity provided by the geotechnical study accompanying any civil works design. The condition defining this restriction was previously established (Equations (20) and (23)).

Percentage of foundation support: Due to the eccentricity of the load system, there is a possibility that the stress distribution at the base of the foundation will generate a negative stress zone. In simple terms, this implies that the foundation would tend to uplift. To ensure that the stresses are properly distributed over the supporting soil, the percentage of the supported section (Equation (24)) must comply with the constraint outlined in Equation (38).

$$\boldsymbol{A \geq 80\%} \tag{38}$$

where:
$\boldsymbol{A}$ = Percentage of foundation supported [%].

Shear strength: From the verification performed above (Equations (31) and (32)), the condition of Equation (39) must be fulfilled:

$$\boldsymbol{\Phi \cdot Vc \geq Vu} \tag{39}$$

where:
$\boldsymbol{\Phi}$ = Shear strength reduction factor of concrete, 0.75.
$\boldsymbol{Vc}$ = Shear strength of concrete section [T].
$\boldsymbol{Vu}$ = Foundation shear request [T].

2.2. Target Function

The objective functions representative of the parameters under study turn out to be linear, and are presented below.

$$\boldsymbol{CMt = CM1 \cdot PM1 + CM2 \cdot PM2} \tag{40}$$

where:
$\boldsymbol{CMt}$ = Total cost of retaining wall [CLP].
$\boldsymbol{CM1}$ = Cost of one cubic meter of concrete [CLP/m^3].
$\boldsymbol{PM1}$ = Total volume of concrete used [m^3].
$\boldsymbol{CM2}$ = Cost of one kilogram of steel [CLP/kg].
$\boldsymbol{PM2}$ = Total kilograms of steel used [kg].

$$\boldsymbol{EMt = EM1 \cdot PM1 + EM2 \cdot PM2} \tag{41}$$

where:
$\boldsymbol{EMt}$ = Total carbon dioxide emissions [T].
$\boldsymbol{EM1}$ = Tons of carbon emitted per cubic meter of concrete [T/m^3].
$\boldsymbol{PM1}$ = Total volume of concrete used [m^3].
$\boldsymbol{EM2}$ = Tons of carbon emitted per kilogram of steel [T/kg].
$\boldsymbol{PM2}$ = Total kilograms of steel used [kg].

$$\boldsymbol{CEMt = (CM1 \cdot PM1 + CM2 \cdot PM2) + EM1 \cdot PM1 + EM2 \cdot PM2} \tag{42}$$

where:
$\boldsymbol{CEMt}$ = Total between the sum of cost and emissions.

3. Techniques to Be Used

In general, design problems involve numerous variables to consider, which may also be of different natures. The combination of multiple options results in a vast number of potential solutions that are impossible to cover manually or iteratively. The need arising from this type of analysis can be addressed through various currently available optimization techniques [19].

Before delving into the optimization techniques applied to the analysis problems relevant to this paper, it is essential to understand what the optimization methods entail. Generally, optimization methods consist of a set of rules and techniques applied to a problem to find the solution that best fits the objective pursued by the process. Optimization methods are divided into two main groups: the first group comprises techniques classified as exact, according to their characteristics [19], which can analyze the entire existing search space and find the best solution for the problem. On the other hand, there are cases where the search space is too large to be explored within a reasonable time frame [19]. In these situations, it is necessary to apply incomplete techniques that focus on analyzing local maxima identified within the function under study.

Another classification method applied to optimization problems focuses on the nature of the decision variables present. Thus, there are continuous optimization problems, meaning their variables represent continuous real spaces. On the other hand, combinatorial optimization problems have variables with integer values or sets of integers. Naturally, a third type of problem involves a mix of both variable types. In these cases, the problem's character is called mixed optimization.

Metaheuristics are iterative processes designed to be applied to any problem type (unlike heuristics, whose configuration is associated with a specific problem type) and, therefore, guide a subordinate heuristic to find an efficient solution in terms of approximation to the global optimum of the problem and the time required to find the proposed solution [20]. Likewise, metaheuristics are subdivided into two groups, depending on the type of solution they provide, and can be based on a single solution or a population of solutions. The above description is graphically represented in Figure 4.

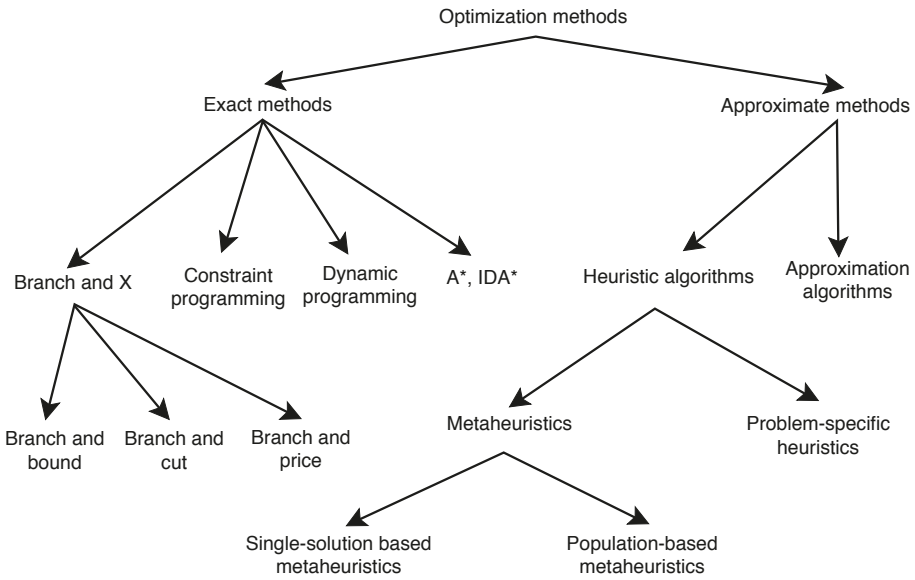

Figure 4. Optimization methods [21].

Regardless of the operation adopted for a metaheuristic, there are general parameters they must follow. First, the problem set must include an objective function, which represents

the aspect of the problem to be optimized. For the purposes of this research, the objective functions to be designed will aim to quantify the costs and carbon dioxide emissions associated with the adopted design.

Once the objective function is defined, two concepts common to any function must be defined: the domain and its constraints. The domain of the objective function directly responds to the values that can be adopted by the variables considered in the problem, which are defined through the constraints. These constraints are conditions (formulated as functions) that limit the problem. All possible solutions that result from the intersection between the constraints of the problem make up the search space that will be considered in the optimization process.

Population-based metaheuristic techniques utilize a structured approach consisting of three "for" loops of iterations, solutions or individuals, and decision dimensions. Under this structure, perturbations to each dimension of the solutions during each iteration are performed through the method indicated in line 5 of Algorithm 1, where $\mathbf{\Delta}$ refers to the characteristic perturbation or movement operators of each technique. As previously mentioned, in this paper, the metaheuristic techniques that have been implemented and discretized to adapt to the presented problem are: the Whale Optimization Algorithm (WOA) [22], the Sine Cosine Algorithm (SCA) [23], and the Grey Wolf Optimizer (GWO) [24]. The general scheme of each population-based metaheuristic is represented in Algorithm 1.

Algorithm 1 General scheme of metaheuristics.

```
1: Initialize a random swarm
2: for iteration (t) do
3:     for solution (i) do
4:         for dimension (d) do
5:             X_{i,d}^{t+1} = X_{i,d}^{t} + Δ
6:         end for
7:     end for
8: end for
```

4. Proposal: Discretization Schemes Selector

The resolution of complex and frequent combinatorial problems in industry is a priority for both academia and industries. A smart scheme selector for discretization is proposed, which integrates existing methods to balance exploration and exploitation, avoiding local optimizations. The balance between exploration and exploitation is a key factor in the performance of a metaheuristic. The method uses an intelligent operator to determine the appropriate discretization scheme at each iteration, to achieve the best quality results.

This proposal is based on the Binarization Schemes Selector (BSS), which has been proposed and utilized in [25–28], where a smart selector at a higher level selects from a set of actions, in this case transfer functions, to better choose how to discretize our continuous variables obtained from the metaheuristic, in order to use them in the discrete domain of our problem.

In this work, Q-Learning (QL) [29] and SARSA [30] are implemented as the intelligent operator of the proposal, which selects the discretization technique to be used based on a reward system, with which it learns in a deterministic manner.

The reward in the RL algorithm is crucial for the good performance of these algorithms; thus, in the literature, there are several methods to calculate rewards. We have implemented the same rewards used in BSS [25,26], which have been proposed in [31,32], which are presented in Equations (43)–(47).

$$withPenalty1 = \begin{cases} +1 & \text{if there is a fitness improvement} \\ -1 & \text{otherwise} \end{cases}, \tag{43}$$

$$withOutPentalty1 = \begin{cases} +1 & \text{if there is a fitness improvement} \\ 0 & \text{otherwise} \end{cases}, \quad (44)$$

$$globalBest = \begin{cases} \dfrac{W}{BestFitness} & \text{if there is a fitness improvement} \\ 0 & \text{otherwise} \end{cases}, \quad (45)$$

$$rootAdaptation = \begin{cases} \sqrt{BestFitness} & \text{if there is a fitness improvement} \\ 0 & \text{otherwise} \end{cases}, \quad (46)$$

and

$$EscalatingMultiplicativeAdaptation = \begin{cases} W \cdot BestFitness & \text{if there is a fitness improvement} \\ 0 & \text{otherwise} \end{cases}, \quad (47)$$

The reward or punishment is judged by the outcome obtained by the performance of the action. Thus, it is important to define which comparison measures will be used to discriminate the outcome. In this work, the comparison measure is the fitness obtained in each iteration of the optimization process, and it is compared with the best fitness obtained. If the fitness improves, the action is rewarded, whereas if the fitness worsens, the action is punished. In this work, two states are defined, which refer to the phases of a metaheuristic: exploration and exploitation. These states were not chosen randomly because, as previously mentioned, the objective of this work is to improve the balance between exploration and exploitation of the metaheuristics to obtain better results. This process is represented in Figure 5.

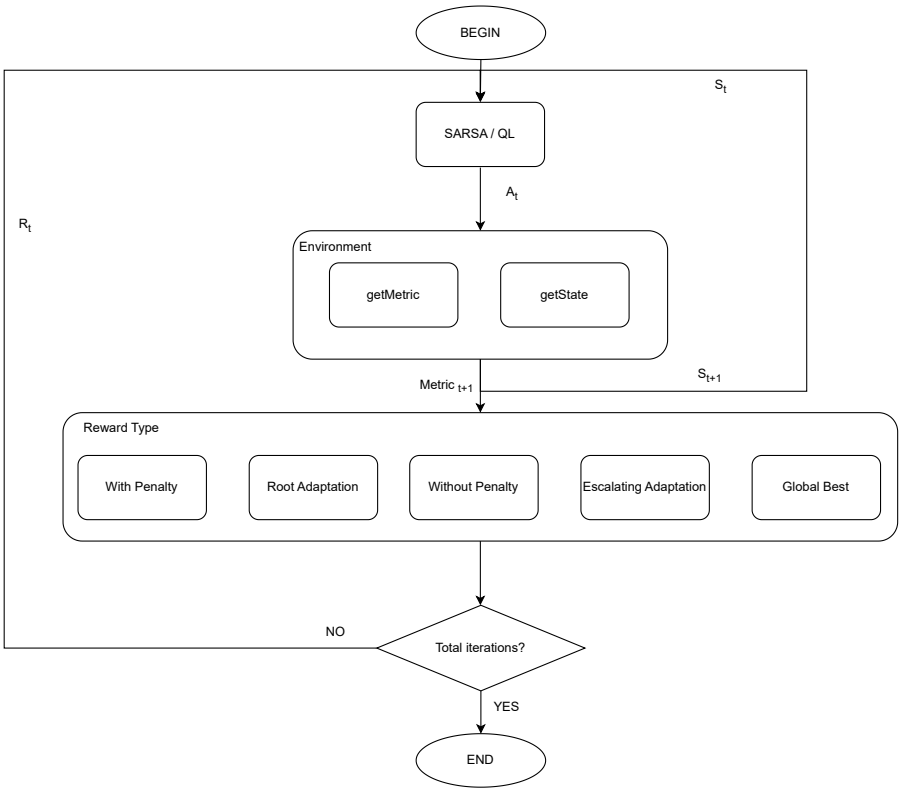

Figure 5. Q-Learning and SARSA scheme for different rewards.

In the literature, different authors [33,34] propose metrics that allow us to quantify the diversity of individuals in population algorithms, where the Dimensional Diversity by

Hussain stands out [35]. Let Div be the diversity of the population at a particular time, and to calculate Div, the following equation is used:

$$Div = \frac{1}{l \cdot n} \sum_{d=1}^{l} \sum_{i=1}^{n} |\bar{x}^d - x_i^d| \tag{48}$$

where $\bar{x}^d$ denotes the average of individuals in dimension d, x_i^d is the value of the i-th individual in dimension d, n is the number of individuals in the population, and l is the size of the dimension of the individuals. One of the methods to estimate exploration and exploitation is proposed by Morales-Castañeda et al. [36], who, based on the quantification of the diversity of a population, proposed a method to estimate exploration and exploitation in terms of percentages. The percentages of exploration (XPL%) and exploitation (XPT%) are calculated as follows:

$$XPL\% = \frac{Div}{Div_{max}} \cdot 100 \tag{49}$$

$$XPT\% = \frac{|Div - Div_{max}|}{Div_{max}} \cdot 100 \tag{50}$$

where Div is the determination of the diversity state given by Equation (49) and Div_{max} denotes the maximum value of the diversity state found throughout the optimization problem. Equations (50) and (51) are generic, so it is possible to use any other metric that calculates the diversity of a population. Therefore, the transition of states will be determined through the following method (Figure 6).

$$next\ state = \begin{cases} Exploration & if\ XPL\% \geq XPT\% \\ Exploitation & if\ XPL\% < XPT\% \end{cases} \tag{51}$$

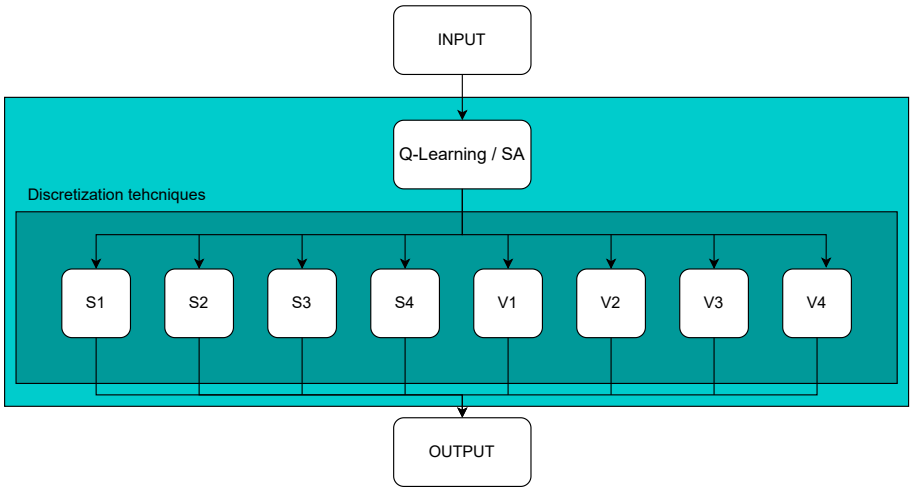

Figure 6. Discretization scheme selector with Q-Learning or SARSA as Smart Operator.

Discretization

There are various ways to transfer continuous values to binaries [37,38], but there is little documentation on discretization. In this proposal, discretization is generated through transfer functions commonly used in two-step binarization. The transfer functions achieve transferring a continuous value to a value in the range of [0, 1]. The discretization proposal is integrated under the general scheme of MH, as presented in Algorithm 2. This discretization function is broken down in Algorithm 3, where the input of the discretization function is the set of solutions, the user-defined parameter $beta$, and the type of transfer function. In the algorithm, for each dimension (line 5), we check if the value of our position $X_{i,d}$ is greater than r_1, which corresponds to a random number between [0, 1] (line 6); if this is met and also the value of $beta > r_2$ another random number between [0, 1] (line 7), then

we update our $X_{i,d}$ to the value of the best solution for that dimension (line 8), but if $beta$ is not greater, then it is updated with a random value (line 10). Otherwise, if the value of $X_{i,d}$ is not greater than r_1, then the element is not updated. Finally (line 17), the discretized value of the solutions X is returned.

Algorithm 2 Discrete general scheme of metaheuristics.

```
1: Initialize a random swarm
2: for iteration (t) do
3:     for solution (i) do
4:         for dimension (d) do
5:             X_{i,d}^{t+1} = X_{i,d}^{t} + Δ
6:         end for
7:     end for
8:     Discretization (X)
9: end for
```

Algorithm 3 Discretization algorithm.

```
1: Function Discretization(X, beta, TF)
2: Initialize r_1 and r_2 as randoms values between [0, 1].
3: XProbability ← appliedTransferFunction(X, TF)
4: for solution (i) do
5:     for dimension (d) do
6:         if X_{i,d} > r_1 then
7:             if beta > r_2 then
8:                 Update X_{i,d} considering the best.
9:             else
10:                Update X_{i,d} with a random value allowed.
11:            end if
12:        else
13:            Do not update the element in X_{i,d}
14:        end if
15:    end for
16: end for
17: return X
```

5. Experimental Results

Three metaheuristics of different classes and complexities have been run for the experimental analysis: SCA, GWO, and WOA. These MH have been tested in 11 instances and run 31 times independently on an i9-10900k, with 32 Gb of RAM and in a Python 3.7 implementation. The extensive experimental comparison has also been carried out on different discretization schemes: on the one hand, on a static scheme using only one of the eight classical transfer functions (S-shaped and V-shaped); and together with the proposal explained in Section 4, using Q-Learning and SARSA as smart selector, each of them evaluating different rewards.

The representative design problem of a retaining wall involves several design variables. Given this situation, and depending on the time required for processing, a list of parameters considered as decision variables will be detailed. Subsequently, these points will take a variable value according to the evaluation to be performed, as determined in the iterative process of the optimization techniques. The following variables used are defined in Table 1.

In order to simplify the representation of results, the main results obtained will be presented, with access to all the results in the open repository https://github.com/joselemusr/DSS-Retaining-walls.

Table 1. Setting parameter.

Variables	Unit	Lower Limit	Upper Limit	Step Size	Possibilities
Concrete strength	Mpa	25	40	5	4
Steel tensil strength	Mpa	280	420	140	2
Width of crowning	m	0.15	0.95	0.01	81
Base width of the wall	m	0.3	1.5	0.01	121
Thickness of the footing	m	0.45	2.0	0.01	156
Density of the structural fill	T/m^3	1.6	2.0	0.1	5

Table 2 presents the nomenclature used to identify each variation of the algorithms, while Tables 3 and 4 present the results obtained by GWO using static schemes based on V-shaped and S-shaped, where this technique has presented the best performance in conjunction with static schemes, where in the first row we can see the version of the algorithm used, in the first column the name of the instance, where the terminations "-C" correspond to those whose objective function calculation is cost-based (Equation (40)), "-E" to those that correspond to CO_2 emissions (Equation (41)) and "-C+E" to the objective function that considers the sum of both (Equation (42)). The second column individualizes the best known value calculated by grid search, and then the three columns are repeated indicating the best value found by the version indicated in the column, the average value of the 31 independent runs and the Relative Percentile Destivation (RPD), which is calculated according to Equation (52). While in intermediate rows the average values for the set of instances using the same objective function are presented.

Table 2. Nomenclature of algorithms.

Name	Reward Types
V1	V-Shaped 1
V2	V-Shaped 2
V3	V-Shaped 3
V4	V-Shaped 4
S1	S-Shaped 1
S2	S-Shaped 2
S3	S-Shaped 3
S4	S-Shaped 4
SA1	With Penalty
SA2	Without Penalty
SA3	Global Best
SA4	Root Adaption
SA5	Scalating Adaption
QL1	With Penalty
QL2	Without Penalty
QL3	Global Best
QL4	Root Adaption
QL5	Scalating Adaption

Table 3. Comparison of the metaheuristics GWO S-shaped.

		S1			S2			S3			S4		
Inst.	Opt.	Best	Avg	RPD	Best	Avg	RPD	Best	Avg	RPD	Best	Avg	RPD
RW300-C	163,992.326	175,838.59	211,292.33	7.22	175,789.67	208,441.35	7.19	188,006.95	212,453.03	14.64	185,972.17	213,282.1	13.4
RW350-C	189,534.031	211,784.64	242,392.1	11.74	201,487.94	238,310.07	6.31	205,963.63	244,063.3	8.67	218,007.71	244,153.67	15.02
RW400-C	214,696.284	230,025.46	276,532.81	7.14	234,785.38	271,573.64	9.36	219,450.0	275,144.37	2.21	232,555.67	277,516.98	8.32
RW450-C	241,096.482	271,731.17	308,495.8	12.71	256,797.33	300,754.16	6.51	270,398.19	312,252.76	12.15	247,671.69	306,537.35	2.73
RW500-C	268,526.177	288,376.68	342,484.67	7.39	288,202.48	339,862.91	7.33	279,819.15	345,778.52	4.21	297,405.15	344,343.23	10.75
RW550-C	307,536.973	324,915.35	382,092.86	5.65	322,283.21	387,920.24	4.79	335,427.48	385,877.51	9.07	322,738.02	370,679.41	4.94
RW600-C	364,409.78	381,612.64	452,607.89	4.72	390,461.48	449,828.17	7.15	377,871.72	436,150.53	3.69	401,195.04	441,721.15	10.09
RW650-C	430,400.866	477,518.43	515,174.31	10.95	454,549.52	506,895.1	5.61	456,260.58	507,368.7	6.01	468,411.9	519,895.88	8.83
RW700-C	507,127.151	547,343.21	602,471.76	7.93	549,909.57	607,197.41	8.44	530,085.84	591,365.14	4.53	534,199.25	598,294.59	5.34
RW750-C	593,353.31	629,727.79	698,312.62	6.13	636,981.05	691,752.62	7.35	628,828.29	696,128.32	5.98	632,268.83	691,309.72	6.56
RW800-C	687,763.656	747,469.72	798,036.46	8.68	729,504.48	802,675.33	6.07	726,214.24	797,384.47	5.59	717,889.37	791,121.94	4.38

Table 3. *Cont.*

		S1			S2			S3			S4		
		389,667.61	439,081.24	8.21	385,522.92	436,837.36	6.92	383,484.19	436,724.24	6.98	387,119.53	436,259.64	8.21
RW300-E	612.204	641.96	753.69	4.86	656.77	763.8	7.28	631.33	763.38	3.12	639.91	766.05	4.53
RW350-E	708.081	756.27	882.66	6.81	808.12	909.04	14.13	778.03	891.86	9.88	762.6	871.11	7.7
RW400-E	802.088	849.79	990.06	5.95	883.34	1018.04	10.13	852.56	984.43	6.29	860.6	998.35	7.29
RW450-E	902.195	977.07	1121.36	8.3	1048.25	1147.36	16.19	912.78	1102.61	1.17	981.13	1099.76	8.75
RW500-E	1007.376	1036.58	1230.59	2.9	1103.16	1240.43	9.51	1085.86	1244.08	7.79	1103.02	1239.52	9.49
RW550-E	1122.621	1197.02	1363.12	6.63	1190.49	1374.09	6.05	1271.84	1369.23	13.29	1241.01	1383.01	10.55
RW600-E	1304.802	1389.11	1602.36	6.46	1391.43	1619.91	6.64	1376.69	1623.79	5.51	1483.51	1603.14	13.7
RW650-E	1545.005	1654.33	1854.43	7.08	1672.47	1837.53	8.25	1588.32	1833.09	2.8	1636.44	1824.26	5.92
RW700-E	1794.782	1955.23	2138.56	8.94	1885.35	2126.44	5.05	1918.4	2159.01	6.89	1846.2	2145.73	2.86
RW750-E	2099.338	2338.08	2516.84	11.37	2243.24	2479.23	6.85	2228.69	2466.35	6.16	2326.47	2522.93	10.82
RW800-E	2443.014	2491.57	2816.65	1.99	2616.19	2849.18	7.09	2697.48	2872.4	10.42	2565.34	2859.6	5.01
		1389.73	1570.03	6.48	1408.98	1578.64	8.83	1394.73	1573.66	6.67	1404.2	1573.95	7.87
RW300-C+E	164,604.53	185,539.96	214,019.57	12.72	179,481.45	208,019.2	9.04	179,206.6	213,775.7	8.87	172,436.99	210,863.58	4.76
RW350-C+E	190,242.112	199,602.67	244,365.08	4.92	203,491.26	246,884.7	6.96	219,538.11	246,767.27	15.4	202,238.98	248,453.56	6.31
RW400-C+E	215,498.372	232,137.79	280,602.84	7.72	230,658.08	273,676.46	7.03	247,064.05	274,698.16	14.65	241,930.5	283,040.63	12.27
RW450-C+E	241,998.678	272,140.43	312,344.84	12.46	266,323.07	309,147.94	10.05	282,508.4	307,997.32	16.74	259,877.32	306,812.62	7.39
RW500-C+E	269,533.553	300,055.55	342,565.29	11.32	295,864.13	335,482.28	9.77	297,761.9	345,023.04	10.47	282,150.29	344,841.59	4.68
RW550-C+E	308,696.291	341,354.54	392,273.06	10.58	340,443.21	390,449.89	10.28	328,562.36	386,558.52	6.44	337,135.95	389,219.89	9.21
RW600-C+E	365,784.894	382,089.49	445,844.69	4.46	390,360.72	451,336.16	6.72	392,607.8	451,473.09	7.33	396,949.96	447,302.6	8.52
RW650-C+E	432,031.377	459,594.11	514,964.67	6.38	466,505.36	517,304.52	7.98	479,176.62	532,639.0	10.91	464,753.64	516,490.98	7.57
RW700-C+E	508,928.933	532,789.38	590,952.6	4.69	550,408.06	609,037.86	8.15	528,020.86	602,847.0	3.75	513,662.21	609,215.53	0.93
RW750-C+E	595,461.955	644,986.79	710,876.08	8.32	622,985.91	695,917.34	4.62	619,227.4	683,463.27	3.99	622,615.54	700,706.2	4.56
RW800-C+E	690,374.634	722,411.98	789,371.57	4.64	730,441.36	789,492.83	5.8	727,830.26	795,986.71	5.43	744,199.77	794,967.2	7.8
		388,427.52	439,834.57	8.02	388,814.78	438,795.38	7.85	391,045.85	440,111.73	9.45	385,268.29	441,083.13	6.73

Table 4. Comparison of the metaheuristics GWO V-shaped.

		V1			V2			V3			V4		
Inst.	Opt.	Best	Avg	RPD	Best	Avg	RPD	Best	Avg	RPD	Best	Avg	RPD
RW300-C	163,992.326	182,558.0	250,774.4	11.32	180,561.07	244,698.22	10.1	180,277.56	255,746.94	9.93	197,594.94	255,313.99	20.49
RW350-C	189,534.031	235,483.99	289,786.83	24.24	236,058.47	296,464.92	24.55	214,982.26	283,628.58	13.43	214,535.82	294,068.78	13.19
RW400-C	214,696.284	256,441.43	311,691.32	19.44	243,710.67	318,303.28	13.51	267,778.96	332,668.32	24.72	239,710.27	328,589.26	11.65
RW450-C	241,096.482	269,111.65	373,108.99	11.62	294,022.51	359,189.16	21.95	280,855.89	388,628.93	16.49	292,597.93	379,517.3	21.36
RW500-C	268,526.177	327,984.08	410,488.65	22.14	298,902.86	411,098.33	11.31	291,171.59	403,594.99	8.43	332,901.71	411,212.61	23.97
RW550-C	307,536.973	371,451.6	459,106.72	20.78	341,735.03	427,316.78	11.12	351,092.89	453,093.61	14.16	349,801.0	448,319.8	13.74
RW600-C	364,409.78	432,595.44	508,425.9	18.71	404,496.27	500,401.85	11.0	415,212.59	501,977.08	13.94	412,811.66	531,849.77	13.28
RW650-C	430,400.866	451,496.13	581,702.33	4.9	454,861.21	596,746.32	5.68	462,874.92	588,805.31	7.55	454,683.35	564,397.16	5.64
RW700-C	507,127.151	566,328.17	680,987.16	11.67	546,341.0	663,127.9	7.73	566,174.43	688,008.95	11.64	538,815.13	664,311.96	6.25
RW750-C	593,353.31	674,866.42	772,500.43	13.74	671,254.82	810,994.06	13.13	677,228.39	778,620.07	14.14	664,697.49	760,457.32	12.02
RW800-C	687,763.656	753,558.36	854,181.21	9.57	757,749.41	907,114.91	10.18	743,863.99	864,887.58	8.16	797,794.43	899,780.3	16.0
		411,079.57	499,341.27	15.28	402,699.39	503,223.25	12.75	404,683.04	503,605.49	12.96	408,722.16	503,438.02	14.33
RW300-E	612.204	659.58	909.38	7.74	664.98	912.97	8.62	698.73	845.7	14.13	658.28	871.39	7.53
RW350-E	708.081	767.18	1061.7	8.35	752.24	1058.21	6.24	821.34	1064.88	16.0	757.65	1034.95	7.0
RW400-E	802.088	927.22	1199.83	15.6	893.96	1167.7	11.45	902.39	1143.52	12.51	887.53	1165.03	10.65
RW450-E	902.195	1003.83	1296.7	11.27	1045.85	1294.51	15.92	949.46	1284.35	5.24	1067.5	1329.86	18.32
RW500-E	1007.376	1170.35	1440.91	16.18	1141.76	1452.99	13.34	1140.6	1438.13	13.22	1123.48	1453.63	11.53
RW550-E	1122.621	1212.53	1613.66	8.01	1267.82	1546.48	12.93	1264.08	1575.83	12.6	1285.56	1626.73	14.51
RW600-E	1304.802	1517.0	1784.2	16.26	1346.81	1881.45	3.22	1416.88	1803.34	8.59	1476.89	1780.07	13.19
RW650-E	1545.005	1754.9	2118.18	13.59	1691.75	2142.13	9.5	1768.66	2130.36	14.48	1703.67	2032.29	10.27
RW700-E	1794.782	2078.11	2441.01	15.79	1935.22	2417.61	7.82	2046.04	2490.55	14.0	2012.62	2431.03	12.14
RW750-E	2099.338	2235.15	2817.56	6.47	2281.91	2719.19	8.7	2306.18	2753.93	9.85	2463.03	2741.43	17.32
RW800-E	2443.014	2763.26	3247.36	13.11	2791.38	3192.71	14.26	2730.05	3244.01	11.75	2627.68	3137.4	7.56
		1462.65	1811.86	12.03	1437.61	1798.72	10.18	1458.58	1797.69	12.03	1460.35	1782.16	11.82
RW300-C+E	164,604.53	189,414.91	256,656.74	15.07	212,808.88	258,560.11	29.28	197,941.42	265,472.25	20.25	191,681.13	255,487.66	16.45
RW350-C+E	190,242.112	226,684.74	289,406.05	19.16	205,267.83	292,174.09	7.9	227,189.95	296,419.26	19.42	215,111.35	298,268.07	13.07
RW400-C+E	215,498.372	249,648.6	320,535.05	15.85	256,337.8	332,853.23	18.95	247,634.93	309,550.68	14.91	251,690.95	325,641.74	16.79
RW450-C+E	241,998.678	266,795.28	368,021.74	10.25	263,973.35	371,100.48	9.08	275,476.78	359,906.58	13.83	292,449.06	365,729.58	20.85
RW500-C+E	269,533.553	319,208.41	396,647.42	18.43	316,227.72	422,102.42	17.32	305,604.13	412,775.82	13.38	300,555.16	397,084.1	11.51
RW550-C+E	308,696.291	345,813.94	434,424.21	12.02	338,561.16	439,581.9	9.67	346,528.45	436,983.83	12.26	375,283.31	460,338.62	21.57
RW600-C+E	365,784.894	391,172.58	511,973.28	6.94	407,135.87	521,235.07	11.3	397,012.72	487,463.91	8.54	389,349.99	513,181.4	6.44
RW650-C+E	432,031.377	500,484.16	576,125.09	15.84	473,065.76	587,658.71	9.5	459,287.25	592,636.18	6.31	511,205.87	587,279.57	18.33
RW700-C+E	508,928.933	570,302.85	685,760.21	12.06	563,174.88	684,648.85	10.66	538,618.15	687,472.3	5.83	568,892.82	693,412.7	11.78
RW750-C+E	595,461.955	676,216.3	773,236.37	13.56	635,506.85	770,898.22	6.73	651,205.08	782,023.88	9.36	638,043.63	775,221.47	7.15
RW800-C+E	690,374.634	766,429.86	887,074.98	11.02	743,847.17	866,593.73	7.75	775,324.71	907,251.95	12.3	740,457.9	903,472.02	7.25
		409,288.33	499,987.38	13.65	401,446.12	504,309.71	12.56	401,983.96	503,450.6	12.4	406,792.83	506,828.81	13.74

Tables 5–10 present the results obtained using the proposed dynamic techniques based on Q-Learning and SARSA.

$$\mathbf{RPD} = \frac{\mathbf{100} \cdot (\boldsymbol{Best} - \boldsymbol{Opt})}{\boldsymbol{Opt}}. \quad (52)$$

Table 5. Comparison of the metaheuristics GWO-SARSA.

		SA1			SA2			SA3			SA4			SA5		
Inst.	Opt.	Best	Avg	RPD	Best	Avg	RPD	Best	Avg	RPD	Best	Avg	RPD	Best	Avg	RPD
RW300-C	163,992.326	175,196.07	240,291.06	6.83	190,461.88	240,768.21	16.14	192,583.95	256,177.38	17.43	196,839.18	255,401.78	20.03	216,562.33	264,100.1	32.06
RW350-C	189,534.031	203,087.74	281,263.13	7.15	212,870.8	280,268.45	12.31	210,817.52	285,790.58	11.23	210,340.34	278,309.36	10.98	204,914.73	284,691.97	8.12
RW400-C	214,696.284	258,788.8	333,047.04	20.54	242,036.31	310,250.08	12.73	263,222.46	332,463.94	22.6	245,698.67	318,591.49	14.44	235,369.05	331,751.44	9.63
RW450-C	241,096.482	246,740.28	360,069.11	2.34	286,128.55	369,184.84	18.68	267,031.65	354,429.31	10.76	290,538.95	370,155.53	20.51	278,411.61	368,804.08	15.48
RW500-C	268,526.177	311,349.28	395,127.49	15.95	333,135.41	420,370.16	24.06	321,064.4	405,607.81	19.57	323,016.44	401,123.74	20.29	313,862.48	404,380.5	16.88
RW550-C	307,536.973	336,252.03	445,129.77	9.34	346,365.66	440,180.83	12.63	355,482.59	434,091.04	15.59	361,102.91	463,967.68	17.42	389,536.95	473,340.33	26.66
RW600-C	364,409.78	401,095.99	499,661.3	10.07	405,588.71	515,558.07	11.3	441,602.08	530,358.24	21.18	422,909.9	510,678.08	16.05	404,582.25	512,612.77	11.02
RW650-C	430,400.866	458,804.21	582,967.98	6.6	488,836.68	592,609.35	13.58	492,186.98	576,837.93	14.36	454,978.62	581,907.37	5.71	485,257.62	608,371.4	12.75
RW700-C	507,127.151	575,813.19	684,980.88	13.54	554,050.72	685,077.06	9.25	574,657.66	692,581.64	13.32	567,477.69	676,364.38	11.9	544,574.66	684,794.22	7.38
RW750-C	593,353.31	651,806.07	775,414.42	9.85	611,414.67	786,125.19	3.04	645,845.55	760,061.05	8.85	628,166.6	791,136.95	5.87	650,375.1	782,284.09	9.61
RW800-C	687,763.656	764,159.62	885,664.16	11.11	719,035.64	875,590.27	4.55	710,899.7	870,215.39	3.36	744,944.09	882,911.76	8.31	752,379.95	909,523.9	9.4
		398,463.03	498,510.58	10.3	399,084.09	501,452.96	12.57	406,854.05	499,874.03	14.39	404,183.04	502,777.1	13.77	406,893.34	511,332.25	14.45
RW300-E	612.204	688.89	915.82	12.53	735.37	862.73	20.12	649.31	917.41	6.06	672.89	882.63	9.91	714.16	907.08	16.65
RW350-E	708.081	814.36	1040.69	15.01	790.0	997.42	11.57	846.06	1014.44	19.49	846.63	1067.25	19.57	797.17	1062.57	12.58
RW400-E	802.088	874.66	1189.78	9.05	951.48	1146.8	18.63	885.43	1153.58	10.39	874.08	1156.67	8.98	895.13	1100.51	11.6
RW450-E	902.195	995.35	1310.04	10.33	958.01	1326.01	6.19	1090.58	1379.05	20.88	1072.61	1291.07	18.89	1004.47	1317.17	11.34
RW500-E	1007.376	1170.04	1458.72	16.15	1071.45	1412.96	6.36	1128.23	1429.47	12.0	1100.51	1352.45	9.25	1116.47	1400.13	10.83
RW550-E	1122.621	1217.65	1531.16	8.46	1206.12	1648.46	7.44	1286.32	1614.5	14.58	1236.62	1648.38	10.15	1248.95	1619.21	11.25
RW600-E	1304.802	1548.61	1869.69	18.69	1543.35	1890.14	18.28	1384.1	1854.52	6.08	1426.58	1812.32	9.33	1578.99	1838.44	21.01
RW650-E	1545.005	1751.98	2099.14	13.4	1754.98	2101.96	13.59	1797.42	2145.75	16.34	1669.69	2098.52	8.07	1765.0	2048.71	14.24
RW700-E	1794.782	2008.91	2415.51	11.93	1949.43	2409.81	8.62	1903.72	2439.5	6.07	2070.63	2538.31	15.37	2209.43	2428.17	23.1
RW750-E	2099.338	2334.47	2776.93	11.2	2319.57	2728.25	10.49	2350.17	2823.53	11.95	2274.59	2760.26	8.35	2426.48	2794.82	15.58
RW800-E	2443.014	2581.15	3093.66	5.65	2614.9	3183.37	7.04	2753.82	3185.19	12.72	2768.04	3206.42	13.3	2687.92	3195.96	10.02
		1453.28	1791.01	12.04	1444.97	1791.63	11.67	1461.38	1814.27	12.41	1455.72	1801.3	11.92	1494.92	1792.07	14.38
RW300-C+E	164,604.53	197,103.77	254,652.15	19.74	164,604.53	251,794.23	0.0	200,235.29	243,330.92	21.65	192,397.52	244,942.0	16.88	198,983.16	263,415.37	20.89
RW350-C+E	190,242.112	205,742.77	295,777.2	8.15	229,743.06	285,923.85	20.76	221,939.8	292,721.98	16.66	215,602.98	295,647.97	13.33	235,526.35	295,891.04	23.8
RW400-C+E	215,498.372	247,338.81	324,435.82	14.78	223,604.65	335,216.13	3.76	233,300.25	316,385.12	8.26	274,532.12	321,902.05	27.39	261,487.63	331,584.94	21.34
RW450-C+E	241,998.678	256,669.92	372,503.2	6.06	263,918.15	378,251.78	9.06	284,180.87	381,454.14	17.43	270,973.96	360,798.33	11.97	277,313.67	369,895.78	14.59
RW500-C+E	269,533.553	287,771.69	398,587.27	6.77	318,733.92	402,187.03	18.25	304,260.04	396,166.19	12.88	329,154.77	406,779.27	22.12	303,022.33	401,482.1	12.42
RW550-C+E	308,696.291	348,667.99	447,725.75	12.95	331,104.97	456,668.02	7.26	340,195.47	450,174.08	10.2	348,179.54	442,063.23	12.79	355,412.73	449,238.6	15.13
RW600-C+E	365,784.894	439,355.55	504,231.19	20.11	420,512.59	501,087.63	14.96	438,608.77	499,684.3	19.91	412,736.13	503,312.77	12.84	381,018.45	512,924.1	4.16
RW650-C+E	432,031.377	494,343.87	593,056.91	14.42	478,256.47	592,585.29	10.7	484,001.98	599,800.75	12.03	481,665.55	581,066.43	11.49	462,419.8	577,629.07	7.03
RW700-C+E	508,928.933	573,299.69	673,059.0	12.65	567,096.46	682,061.35	11.43	587,805.05	674,570.95	15.5	565,677.47	673,489.21	11.15	578,495.41	681,417.61	13.67
RW750-C+E	595,461.955	664,560.38	793,803.33	11.6	685,914.43	782,065.86	15.19	653,984.87	765,896.12	9.83	641,280.95	786,801.82	7.69	680,615.86	787,048.52	14.3
RW800-C+E	690,374.634	778,611.38	884,246.73	12.78	733,278.57	875,246.18	6.21	749,760.94	881,804.84	8.6	785,722.86	878,414.05	13.81	754,160.86	863,339.01	9.24
		408,496.89	503,825.32	12.73	401,524.35	503,917.03	10.69	408,933.94	500,180.85	13.9	410,720.35	499,565.19	14.68	408,041.48	503,078.74	14.23

Table 6. Comparison of the metaheuristics WOA-SARSA.

		SA1			**SA2**			**SA3**			**SA4**			**SA5**		
Inst.	Opt.	Best	Avg	RPD	Best	Avg	RPD	Best	Avg	RPD	Best	Avg	RPD	Best	Avg	RPD
RW300-C	163,992.326	174,401.85	207,029.1	6.35	167,693.67	206,464.53	2.26	177,799.48	203,958.3	8.42	176,090.82	210,441.84	7.38	172,075.6	207,216.98	4.93
RW350-C	189,534.031	215,236.86	247,721.69	13.56	207,641.36	241,905.55	9.55	197,658.72	244,658.14	4.29	201,255.16	244,411.26	6.18	198,809.45	248,571.28	4.89
RW400-C	214,696.284	233,655.98	277,485.21	8.83	237,279.59	274,184.6	10.52	243,725.11	279,525.08	13.52	247,387.97	279,426.94	15.23	220,850.79	274,863.6	2.87
RW450-C	241,096.482	254,615.8	304,331.36	5.61	266,160.75	311,813.82	10.4	255,681.45	302,243.06	6.05	258,985.05	304,964.45	7.42	246,412.94	305,338.33	2.21
RW500-C	268,526.177	289,994.65	330,993.01	7.99	309,115.38	347,294.56	15.12	315,287.02	347,787.85	17.41	291,863.8	330,424.63	8.69	286,939.71	341,076.69	6.86
RW550-C	307,536.973	320,202.08	380,843.12	4.12	325,913.34	379,485.88	5.98	337,056.39	380,688.05	9.6	329,631.25	389,187.29	7.18	336,706.88	386,894.3	9.49
RW600-C	364,409.78	409,154.41	462,149.01	12.28	397,224.77	453,183.43	9.0	395,937.23	444,542.84	8.65	413,376.31	454,884.63	13.44	404,343.26	449,467.23	10.96
RW650-C	430,400.866	454,719.22	525,030.05	5.65	481,048.56	530,789.22	11.77	472,013.02	528,236.95	9.67	476,062.98	525,748.47	10.61	482,424.65	532,537.15	12.09
RW700-C	507,127.151	531,392.11	620,977.14	4.78	524,947.85	615,962.48	3.51	551,926.18	610,816.7	8.83	548,174.2	617,980.64	8.09	534,076.8	619,482.1	5.31
RW750-C	593,353.31	626,565.97	710,680.86	5.6	619,245.39	702,241.1	4.36	619,168.27	707,639.74	4.35	615,416.51	703,534.96	3.72	619,412.94	712,491.68	4.39
RW800-C	687,763.656	730,742.66	819,292.53	6.25	765,546.44	829,570.55	11.31	735,548.58	810,045.45	6.95	739,563.3	821,056.54	7.53	728,891.84	811,673.87	5.98
		385,516.51	444,230.28	7.37	391,074.28	444,808.7	8.53	391,072.86	441,831.11	8.89	390,709.76	443,823.79	8.68	384,631.35	444,510.29	6.36
RW300-E	612.204	663.98	760.41	8.46	644.76	772.53	5.32	630.17	756.58	2.93	623.88	761.46	1.91	637.36	763.04	4.11
RW350-E	708.081	759.42	883.15	7.25	736.14	856.49	3.96	743.98	884.01	5.07	766.93	882.5	8.31	742.38	860.32	4.84
RW400-E	802.088	872.46	990.58	8.77	848.82	999.5	5.83	820.3	993.31	2.27	823.17	1008.7	2.63	867.04	988.42	8.1
RW450-E	902.195	947.01	1098.09	4.97	951.08	1101.75	5.42	935.97	1099.21	3.74	995.66	1119.5	10.36	943.81	1097.13	4.61
RW500-E	1007.376	1043.18	1241.94	3.55	1080.83	1237.65	7.29	1072.62	1215.82	6.48	1119.17	1264.68	11.1	1059.68	1224.23	5.19
RW550-E	1122.621	1144.32	1384.74	1.93	1221.65	1368.57	8.82	1238.14	1367.13	10.29	1197.19	1390.5	6.64	1185.22	1392.82	5.58
RW600-E	1304.802	1419.08	1616.32	8.76	1373.27	1599.68	5.25	1391.69	1594.11	6.66	1394.72	1614.18	6.89	1406.36	1600.15	7.78
RW650-E	1545.005	1665.69	1887.99	7.81	1651.93	1861.29	6.92	1604.84	1874.46	3.87	1673.72	1884.58	8.33	1675.24	1904.6	8.43
RW700-E	1794.782	1962.45	2214.69	9.34	1982.95	2214.33	10.48	1954.1	2174.09	8.88	1902.16	2191.95	5.98	1945.27	2209.72	8.38
RW750-E	2099.338	2264.7	2571.84	7.88	2292.04	2575.99	9.18	2212.81	2539.55	5.41	2221.2	2521.84	5.8	2250.96	2552.38	7.22
RW800-E	2443.014	2663.93	2953.13	9.04	2722.65	2937.81	11.45	2823.38	3046.43	15.57	2605.43	2923.0	6.65	2629.9	2913.56	7.65
		1400.57	1600.26	7.07	1409.65	1593.24	7.27	1402.55	1594.97	6.47	1393.02	1596.63	6.78	1394.84	1591.49	6.54
RW300-C+E	164,604.53	168,658.98	212,727.19	2.46	176,444.67	205,058.94	7.19	173,056.52	214,816.59	5.13	182,264.77	209,180.81	10.73	183,163.86	217,919.74	11.28
RW350-C+E	190,242.112	208,636.51	250,315.97	9.67	201,523.94	243,996.67	5.93	196,473.6	248,565.95	3.28	201,849.61	240,120.29	6.1	209,651.55	248,083.69	10.2
RW400-C+E	215,498.372	236,614.01	275,954.32	9.8	239,632.13	277,064.09	11.2	224,193.97	265,672.91	4.04	229,261.36	271,977.58	6.39	244,633.69	283,644.99	13.52
RW450-C+E	241,998.678	270,957.25	310,023.22	11.97	257,290.6	306,282.91	6.32	280,742.96	320,823.27	16.01	256,252.7	311,883.58	5.89	261,084.72	313,347.59	7.89
RW500-C+E	269,533.553	308,085.44	342,097.22	14.3	293,506.55	348,175.63	8.89	281,713.39	343,204.09	4.52	296,651.36	346,621.13	10.06	282,994.86	331,343.68	4.99
RW550-C+E	308,696.291	342,032.54	392,228.11	10.8	329,122.6	375,492.42	6.62	335,151.94	388,785.13	8.57	337,425.85	382,851.06	9.31	325,039.5	382,216.95	5.29
RW600-C+E	365,784.894	377,921.76	443,097.53	3.32	402,061.9	464,050.7	9.92	386,279.94	443,721.28	5.6	392,853.36	446,311.8	7.4	390,294.82	457,974.88	6.7
RW650-C+E	432,031.377	469,187.01	525,056.83	8.6	464,313.64	526,829.5	7.47	464,800.5	525,976.15	7.58	463,004.0	519,128.6	7.17	473,514.3	533,492.6	9.6
RW700-C+E	508,928.933	558,249.29	613,632.89	9.69	567,040.8	612,672.63	11.42	543,066.2	622,176.4	6.71	546,718.92	613,544.22	7.43	554,975.79	611,984.05	9.05
RW750-C+E	595,461.955	654,041.06	710,449.31	9.84	647,750.72	726,656.72	8.78	645,172.05	713,194.58	8.35	629,497.71	722,580.29	5.72	646,497.24	717,550.24	8.57
RW800-C+E	690,374.634	746,445.96	821,317.48	8.12	758,672.75	821,534.7	9.89	728,552.96	812,729.46	5.53	738,894.47	821,098.05	7.03	740,506.94	826,309.19	7.26
		394,620.89	445,172.73	8.96	394,305.48	446,164.99	8.51	387,200.37	445,424.16	6.85	388,606.74	444,117.95	7.57	392,032.48	447,624.33	8.58

Table 7. Comparison of the metaheuristics SCA-SARSA.

		SA1			**SA2**			**SA3**			**SA4**			**SA5**		
Inst.	Opt.	Best	Avg	RPD	Best	Avg	RPD	Best	Avg	RPD	Best	Avg	RPD	Best	Avg	RPD
RW300-C	163,992.326	177,137.67	224,260.78	8.02	180,792.13	220,153.89	10.24	182,743.3	219,209.54	11.43	177,206.82	234,269.03	8.06	182,686.29	241,289.47	11.4
RW350-C	189,534.031	208,138.12	264,710.41	9.82	202,664.92	269,416.08	6.93	201,953.08	262,367.93	6.55	207,615.0	269,509.83	9.54	213,815.68	264,199.64	12.81
RW400-C	214,696.284	225,119.78	291,785.74	4.85	240,342.74	304,398.82	11.95	232,461.48	300,241.53	8.27	246,457.28	296,371.99	14.79	233,717.84	302,323.41	8.86
RW450-C	241,096.482	278,095.59	323,782.93	15.35	269,654.9	342,157.21	11.85	252,396.03	332,456.51	4.69	271,024.1	334,596.22	12.41	281,990.47	339,022.7	16.96
RW500-C	268,526.177	288,284.59	368,227.63	7.36	273,124.46	370,022.32	1.71	297,248.48	362,742.78	10.7	281,004.63	363,934.9	4.65	305,071.97	373,895.89	13.61
RW550-C	307,536.973	338,844.89	392,264.2	10.18	323,906.32	416,680.35	5.32	333,697.21	404,026.04	8.51	343,922.52	410,328.48	11.83	313,331.75	404,645.32	1.88
RW600-C	364,409.78	373,922.98	479,795.73	2.61	401,552.2	474,158.07	10.19	403,437.77	462,371.55	10.71	387,705.3	479,860.42	6.39	407,833.99	475,558.99	11.92
RW650-C	430,400.866	464,199.96	541,047.14	7.85	478,302.01	545,685.64	11.13	484,950.95	547,191.46	12.67	460,644.89	531,631.54	7.03	462,758.53	545,869.92	7.52
RW700-C	507,127.151	524,925.0	615,145.01	3.51	550,871.52	620,348.25	8.63	540,526.5	617,313.87	6.59	546,543.27	629,484.51	7.77	549,550.4	615,424.43	8.37
RW750-C	593,353.31	638,144.22	729,317.37	7.55	633,964.23	713,740.48	6.84	603,561.86	724,955.72	1.72	602,775.81	715,782.64	1.59	635,394.83	730,607.54	7.09
RW800-C	687,763.656	743,476.16	827,808.92	8.1	758,914.12	840,577.68	10.35	731,345.26	826,673.89	6.34	768,513.66	835,314.43	11.74	752,583.06	853,668.89	9.42
		387,299.0	459,831.44	7.75	392,189.96	465,212.62	8.65	387,665.63	459,959.17	8.02	390,310.3	463,734.91	8.71	394,430.44	467,864.2	9.99
RW300-E	612.204	640.94	796.13	4.69	710.79	815.84	16.1	659.82	829.18	7.78	673.18	814.48	9.96	668.83	820.84	9.25
RW350-E	708.081	787.69	931.19	11.24	778.37	936.24	9.93	797.53	972.38	12.63	768.86	958.7	8.58	761.78	934.74	7.58
RW400-E	802.088	837.28	1044.97	4.39	854.25	1097.08	6.5	828.13	1082.06	3.25	877.33	1102.57	9.38	818.45	1038.65	2.04
RW450-E	902.195	952.68	1167.46	5.6	926.25	1181.68	2.67	1003.99	1142.18	11.28	942.58	1204.58	4.48	922.21	1241.86	2.22
RW500-E	1007.376	1057.46	1333.02	4.97	1119.65	1287.35	11.15	1111.76	1273.86	10.36	1103.8	1330.23	9.57	1060.32	1300.37	5.26
RW550-E	1122.621	1171.26	1412.38	4.33	1241.98	1543.5	10.63	1194.15	1502.52	6.37	1204.02	1449.21	7.25	1256.45	1449.66	11.92
RW600-E	1304.802	1479.84	1705.17	13.41	1422.84	1709.0	9.05	1440.0	1693.05	10.36	1422.57	1742.77	9.03	1416.34	1665.51	8.55
RW650-E	1545.005	1673.44	1980.37	8.31	1657.88	1909.21	7.31	1712.47	2022.58	10.84	1760.84	1985.75	13.97	1710.21	1947.59	10.69
RW700-E	1794.782	2009.14	2256.78	11.94	1840.68	2215.83	2.56	1962.28	2304.68	9.33	1978.56	2249.0	10.24	2003.18	2266.59	11.61
RW750-E	2099.338	2277.72	2671.58	8.5	2323.97	2620.33	10.7	2300.57	2612.05	9.59	2300.95	2604.42	9.6	2236.35	2586.29	6.53
RW800-E	2443.014	2515.07	3020.55	2.95	2641.07	3107.25	8.11	2558.83	3070.18	4.74	2776.85	3050.21	13.66	2553.02	2943.3	4.5
		1400.23	1665.42	7.3	1410.7	1674.85	8.61	1415.41	1682.25	8.78	1437.23	1681.08	9.61	1400.65	1654.13	7.29
RW300-C+E	164,604.53	191,743.67	226,511.74	16.49	181,596.71	230,891.6	10.32	180,976.64	234,010.52	9.95	195,423.7	231,432.35	18.72	175,920.48	237,062.88	6.87
RW350-C+E	190,242.112	222,804.94	273,797.72	17.12	218,336.27	258,386.31	14.77	211,417.37	257,122.1	11.13	205,444.15	267,836.18	7.99	214,776.6	255,807.43	12.9
RW400-C+E	215,498.372	240,584.89	297,668.72	11.64	244,314.74	295,141.6	13.37	243,681.08	297,702.5	13.08	244,374.07	304,452.39	13.4	235,532.13	292,965.37	9.3
RW450-C+E	241,998.678	260,571.64	319,689.99	7.67	275,969.78	351,627.98	14.04	270,337.65	324,947.75	11.71	266,661.81	329,405.83	10.19	282,489.65	333,755.77	16.73
RW500-C+E	269,533.553	294,207.44	362,719.28	9.15	292,405.83	382,757.22	8.49	308,064.16	368,159.31	14.3	287,093.28	354,839.89	6.51	304,824.33	385,826.92	13.09
RW550-C+E	308,696.291	338,155.87	407,161.79	9.54	332,058.08	397,247.0	7.57	347,456.95	403,418.66	12.56	345,919.22	409,010.58	12.06	350,825.92	411,122.26	13.65
RW600-C+E	365,784.894	394,037.68	474,484.14	7.72	392,325.69	466,762.67	7.26	396,665.15	473,394.71	8.44	371,338.58	464,602.41	1.52	395,092.17	466,928.06	8.01
RW650-C+E	432,031.377	465,552.5	537,368.9	7.76	463,945.52	559,430.69	7.39	450,055.53	540,802.93	4.17	489,920.9	544,086.45	13.4	453,510.51	536,280.48	4.97
RW700-C+E	508,928.933	539,416.34	611,180.39	5.99	539,475.72	656,532.65	6.0	550,291.12	637,226.63	8.13	547,315.59	648,959.9	7.54	528,800.69	625,629.17	3.9
RW750-C+E	595,461.955	631,156.69	725,192.7	5.99	658,561.1	716,445.05	10.6	664,568.92	723,674.37	11.61	646,749.89	734,467.67	8.61	618,807.48	722,541.13	3.92
RW800-C+E	690,374.634	727,997.55	831,451.81	5.45	750,169.78	836,083.2	8.66	727,071.28	820,679.47	5.32	733,179.58	843,869.81	6.2	731,795.7	834,718.22	6.0
		391,475.38	460,657.02	9.5	395,378.11	468,300.54	9.86	395,507.8	461,921.72	10.04	393,947.34	466,633.04	9.65	390,215.97	463,876.15	9.03

Table 8. Comparison of the metaheuristics GWO-Q-Learning.

		QL1			QL2			QL3			QL4			QL5		
Inst.	Opt.	Best	Avg	RPD	Best	Avg	RPD	Best	Avg	RPD	Best	Avg	RPD	Best	Avg	RPD
RW300-C	163,992.326	197,892.79	257,638.59	20.67	206,934.24	250,757.28	26.19	203,568.86	259,082.85	24.13	172,736.65	246,105.69	5.33	177,495.95	249,255.49	8.23
RW350-C	189,534.031	217,737.04	283,106.81	14.88	220,049.1	297,439.17	16.1	204,505.07	278,060.04	7.9	235,434.81	284,381.8	24.22	220,907.56	282,927.24	16.55
RW400-C	214,696.284	223,424.83	322,090.81	4.07	232,013.55	314,385.08	8.07	244,249.75	335,600.85	13.77	261,056.46	331,349.56	21.59	239,791.93	328,211.09	11.69
RW450-C	241,096.482	262,957.21	360,952.11	9.07	272,207.68	360,699.95	12.9	299,063.03	385,244.17	24.04	284,841.37	350,877.47	18.14	306,208.81	362,661.94	27.01
RW500-C	268,526.177	329,483.68	405,237.1	22.7	303,501.72	412,561.15	13.03	325,572.9	397,863.76	21.24	287,946.31	397,195.24	7.23	325,128.92	404,403.3	21.08
RW550-C	307,536.973	344,772.37	457,779.42	12.11	358,873.14	451,495.97	16.69	359,432.96	447,394.56	16.87	350,131.68	445,150.53	13.85	358,348.11	458,279.49	16.52
RW600-C	364,409.78	396,926.79	506,912.79	8.92	396,683.7	522,148.78	8.86	391,759.26	504,070.17	7.51	424,489.24	518,622.63	16.49	425,651.66	513,125.41	16.81
RW650-C	430,400.866	519,592.66	588,642.14	20.72	493,303.76	596,264.8	14.61	475,749.49	583,199.11	10.54	480,635.17	579,539.01	11.67	456,432.52	574,790.37	6.05
RW700-C	507,127.151	548,096.45	668,941.43	8.08	558,827.52	667,943.89	10.19	577,373.47	692,838.03	13.85	568,190.05	671,328.82	12.04	562,920.67	689,582.48	11.0
RW750-C	593,353.31	695,346.84	794,320.97	17.19	637,025.4	773,971.02	7.36	649,041.8	777,650.2	9.39	653,562.37	770,229.26	10.15	655,015.04	776,344.95	10.39
RW800-C	687,763.656	746,206.77	908,642.62	8.5	741,355.73	870,059.87	7.79	754,644.88	890,950.53	9.72	755,281.03	897,244.36	9.82	779,030.16	884,149.4	13.27
		407,494.31	504,933.16	13.36	401,888.69	501,611.54	12.89	407,723.77	504,723.12	14.45	406,755.01	499,274.94	13.68	409,721.03	502,157.38	14.42
RW300-E	612.204	651.3	910.98	6.39	723.88	878.64	18.24	747.7	954.87	22.13	665.48	919.97	8.7	638.55	876.09	4.3
RW350-E	708.081	826.31	1025.29	16.7	775.07	1079.81	9.46	788.2	1055.87	11.31	850.66	1043.48	20.14	792.36	1036.66	11.9
RW400-E	802.088	934.37	1173.44	16.49	929.92	1147.64	15.94	994.44	1202.56	23.98	936.8	1186.46	16.8	870.25	1218.5	8.5
RW450-E	902.195	1066.1	1345.53	18.17	963.6	1318.08	6.81	970.66	1283.31	7.59	1055.42	1358.65	16.98	1007.98	1317.88	11.73
RW500-E	1007.376	1087.77	1482.4	7.98	1115.68	1494.89	10.75	1048.32	1422.36	4.06	1171.28	1420.02	16.27	1175.56	1443.05	16.7
RW550-E	1122.621	1327.25	1627.9	18.23	1176.47	1625.49	4.8	1202.67	1657.65	7.13	1351.81	1598.86	20.42	1194.37	1535.23	6.39
RW600-E	1304.802	1445.11	1812.71	10.75	1491.64	1852.81	14.32	1519.54	1833.87	16.46	1414.77	1843.88	8.43	1488.03	1850.23	14.04
RW650-E	1545.005	1653.79	2072.22	7.04	1810.77	2123.03	17.2	1655.41	2078.2	7.15	1768.8	2164.97	14.49	1707.91	2187.33	10.54
RW700-E	1794.782	1983.98	2408.77	10.54	1984.53	2458.17	10.57	2021.71	2394.12	12.64	1989.86	2449.14	10.87	2100.89	2411.72	17.06
RW750-E	2099.338	2449.23	2859.24	16.67	2175.81	2753.22	3.64	2375.99	2697.55	13.18	2338.62	2735.78	11.4	2495.79	2800.35	18.88
RW800-E	2443.014	2610.96	3175.52	6.87	2638.71	3241.34	8.01	2627.71	3143.76	7.56	2748.99	3135.94	12.52	2743.37	3198.12	12.29
		1457.83	1808.55	12.35	1435.1	1815.74	10.89	1450.21	1793.1	12.11	1481.14	1805.2	14.27	1474.1	1806.83	12.03
RW300-C+E	164,604.53	185,796.05	243,809.71	12.87	202,162.53	243,757.6	22.82	183,278.96	260,952.12	11.35	183,137.41	255,109.24	11.26	183,496.26	250,417.07	11.48
RW350-C+E	190,242.112	212,734.69	274,328.31	11.82	199,602.67	289,577.45	4.92	209,225.59	282,636.96	9.98	226,184.6	285,846.74	18.89	211,233.18	301,547.46	11.03
RW400-C+E	215,498.372	255,409.44	328,338.0	18.52	259,207.31	332,639.78	20.28	266,267.21	326,303.42	23.56	246,328.62	321,452.6	14.31	228,861.37	317,274.1	6.2
RW450-C+E	241,998.678	293,601.11	378,530.34	21.32	290,544.7	361,951.9	20.06	267,252.84	351,208.7	10.44	283,005.24	359,741.31	16.94	271,356.09	368,247.58	12.13
RW500-C+E	269,533.553	326,651.82	399,949.35	21.19	348,778.15	424,617.96	29.4	317,728.91	394,358.37	17.88	305,303.79	393,611.82	13.27	294,511.1	396,863.42	9.27
RW550-C+E	308,696.291	355,227.94	436,084.62	15.07	367,449.96	454,832.35	19.03	343,368.19	455,531.22	11.23	347,258.97	440,703.81	12.49	357,505.5	457,301.15	15.81
RW600-C+E	365,784.894	393,744.02	503,790.36	7.64	401,591.38	496,164.09	9.79	448,987.03	529,621.12	22.75	386,989.19	505,689.04	5.8	419,763.84	535,334.0	14.76
RW650-C+E	432,031.377	510,668.26	600,033.77	18.2	483,963.46	586,909.4	12.02	488,789.99	574,895.06	13.14	473,926.61	579,769.97	9.7	488,983.79	578,679.85	13.18
RW700-C+E	508,928.933	585,704.28	689,313.24	15.09	545,300.46	679,389.03	7.15	572,869.47	668,470.81	12.56	548,274.64	680,069.01	7.73	552,305.67	678,685.23	8.52
RW750-C+E	595,461.955	619,243.47	758,516.92	3.99	633,591.06	776,961.42	6.4	646,726.63	772,444.18	8.61	672,807.9	792,451.82	12.99	660,934.61	785,924.37	11.0
RW800-C+E	690,374.634	763,266.05	877,440.83	10.56	737,978.01	894,599.76	6.9	741,107.15	899,987.75	7.35	762,147.16	859,215.5	10.4	743,333.62	879,484.62	7.67
		409,277.01	499,103.22	14.21	406,379.06	503,763.7	14.43	407,782.0	501,491.79	13.53	403,214.92	497,605.53	12.16	401,116.82	504,523.53	11.0

Table 9. Comparison of the metaheuristics WOA-Q-Learning.

		QL1			QL2			QL3			QL4			QL5		
Inst.	Opt.	Best	Avg	RPD	Best	Avg	RPD	Best	Avg	RPD	Best	Avg	RPD	Best	Avg	RPD
RW300-C	163,992.326	179,177.48	209,734.64	9.26	173,509.5	203,596.77	5.8	170,706.86	207,633.81	4.09	185,312.43	213,852.83	13.0	163,992.33	205,627.47	0.0
RW350-C	189,534.031	205,752.81	241,320.7	8.56	203,569.89	238,574.78	7.41	211,172.74	242,262.91	11.42	213,805.06	246,293.15	12.81	209,309.7	246,491.78	10.43
RW400-C	214,696.284	227,324.11	276,268.73	5.88	227,531.0	283,235.62	5.98	223,522.86	275,191.01	4.11	245,809.55	273,823.44	14.49	225,086.49	278,784.69	4.84
RW450-C	241,096.482	264,259.18	302,763.29	9.61	264,773.19	317,063.15	9.82	261,357.87	307,262.55	8.4	258,086.05	302,749.37	7.05	250,145.73	299,479.43	3.75
RW500-C	268,526.177	304,701.79	343,712.18	13.47	298,170.23	344,511.81	11.04	298,629.9	344,978.57	11.21	273,665.15	344,935.49	1.91	287,240.58	339,252.49	6.97
RW550-C	307,536.973	332,096.06	375,328.34	7.99	323,977.91	378,769.29	5.35	315,787.31	376,502.94	2.68	340,849.45	390,008.5	10.83	325,698.68	383,431.79	5.91
RW600-C	364,409.78	372,143.69	440,450.72	2.12	398,219.72	448,192.85	9.28	392,734.46	457,851.82	7.77	378,012.35	449,357.08	3.73	396,509.26	447,343.62	8.81
RW650-C	430,400.866	458,835.67	523,675.6	6.61	457,330.96	530,599.28	6.26	462,444.22	537,511.2	7.45	465,973.89	521,804.69	8.27	455,764.04	519,138.09	5.89
RW700-C	507,127.151	530,806.81	608,609.13	4.67	540,729.04	619,650.83	6.63	533,396.7	624,480.25	5.18	542,663.49	608,858.11	7.01	566,906.53	625,117.17	11.79
RW750-C	593,353.31	669,062.95	721,546.44	12.76	640,694.98	710,998.3	7.98	621,468.68	713,327.48	4.74	630,088.45	710,117.84	6.19	644,004.67	720,258.11	8.54
RW800-C	687,763.656	731,559.18	821,138.33	6.37	741,347.04	811,804.51	7.79	741,720.21	833,808.12	7.85	739,752.64	823,544.81	7.56	736,943.23	823,397.66	7.15
		388,701.79	442,231.65	7.94	388,168.5	444,272.47	7.58	384,812.89	447,346.42	6.81	388,547.14	444,122.3	8.44	387,418.29	444,392.94	6.73
RW300-E	612.204	681.66	770.1	11.35	651.95	747.04	6.49	651.75	753.22	6.46	626.13	766.51	2.27	665.47	763.41	8.7
RW350-E	708.081	755.94	886.8	6.76	777.37	877.05	9.79	771.3	897.6	8.93	743.82	876.41	5.05	761.48	881.68	7.54
RW400-E	802.088	892.45	998.25	11.27	824.23	999.57	2.76	870.41	985.51	8.52	835.8	1012.89	4.2	853.19	975.38	6.37
RW450-E	902.195	956.45	1112.15	6.01	911.56	1099.19	1.04	941.79	1122.56	4.39	951.14	1113.93	5.43	961.24	1114.9	6.54
RW500-E	1007.376	1048.32	1270.49	4.06	1044.44	1238.39	3.68	1076.63	1233.77	6.87	1055.8	1247.12	4.81	1105.15	1245.1	9.71
RW550-E	1122.621	1230.99	1401.38	9.65	1227.75	1400.52	9.36	1210.35	1382.88	7.81	1170.27	1352.35	4.24	1189.31	1381.38	5.94
RW600-E	1304.802	1433.3	1584.19	9.85	1443.55	1584.51	10.63	1466.49	1649.07	12.39	1364.98	1576.17	4.61	1401.96	1632.68	7.45
RW650-E	1545.005	1651.73	1899.73	6.91	1674.59	1890.45	8.39	1681.7	1897.8	8.85	1714.19	1895.53	10.95	1665.06	1869.05	7.77
RW700-E	1794.782	1905.46	2178.49	6.17	1893.02	2183.6	5.47	1950.12	2182.28	8.65	1858.8	2161.97	3.57	1969.88	2171.85	9.76
RW750-E	2099.338	2249.11	2547.13	7.13	2236.64	2555.99	6.54	2294.51	2553.94	9.3	2301.72	2599.84	9.64	2310.63	2562.96	10.06
RW800-E	2443.014	2610.63	2945.13	6.86	2669.1	2954.83	9.25	2565.6	2948.68	5.02	2641.95	2973.11	8.14	2631.57	2958.9	7.72
		1401.46	1599.44	7.82	1395.84	1593.74	6.67	1407.33	1600.66	7.93	1387.69	1597.8	5.72	1410.45	1596.12	7.96
RW300-C+E	164,604.53	192,163.04	217,195.43	16.74	180,503.12	208,418.99	9.66	175,837.81	210,338.41	6.82	184,342.08	211,341.16	11.99	180,867.27	208,979.87	9.88
RW350-C+E	190,242.112	205,706.7	244,438.78	8.13	198,685.25	235,924.1	4.44	212,783.52	245,577.84	11.85	204,786.43	246,370.21	7.65	212,304.11	243,465.48	11.6
RW400-C+E	215,498.372	233,881.15	278,527.63	8.53	232,257.03	272,418.78	7.78	240,999.43	282,502.8	11.83	235,011.55	273,551.43	9.05	239,611.42	279,434.38	11.19
RW450-C+E	241,998.678	269,162.46	309,912.24	11.22	251,926.58	313,113.95	4.1	262,562.55	310,494.65	8.5	250,607.99	313,224.14	3.56	266,679.25	316,270.77	10.2
RW500-C+E	269,533.553	290,900.58	345,075.04	7.93	293,399.22	341,136.74	8.85	284,434.62	329,608.51	5.53	281,154.2	334,725.13	4.31	290,972.35	346,654.16	7.95
RW550-C+E	308,696.291	324,837.6	378,041.39	5.23	333,413.4	388,181.0	8.01	342,165.68	386,204.37	10.84	339,325.66	390,623.98	9.92	345,612.72	386,947.89	11.96
RW600-C+E	365,784.894	392,542.47	448,391.81	7.32	408,737.83	446,852.2	11.74	390,921.15	450,464.34	6.87	400,027.15	447,415.89	9.36	397,653.18	445,113.56	8.71
RW650-C+E	432,031.377	453,990.37	521,024.94	5.08	462,994.09	520,041.75	7.17	451,717.44	521,551.42	4.56	447,965.11	523,135.28	3.69	458,944.13	533,686.33	6.23
RW700-C+E	508,928.933	541,769.0	628,241.11	6.45	537,410.91	622,687.44	5.6	551,167.05	626,569.19	8.3	543,383.44	613,361.01	6.77	563,812.97	614,530.51	10.78
RW750-C+E	595,461.955	667,404.79	716,299.26	12.08	630,451.77	718,923.87	5.88	638,116.46	702,900.44	7.16	621,906.63	717,452.25	4.44	635,051.81	706,863.81	6.65
RW800-C+E	690,374.634	740,820.65	813,583.22	7.31	730,350.91	820,324.92	5.79	738,857.26	826,262.18	7.02	747,392.85	827,572.44	8.26	746,636.42	831,011.81	8.15
		392,107.16	445,520.99	8.73	387,284.56	444,365.79	7.18	389,960.27	444,770.38	8.12	386,900.28	445,342.99	7.18	394,376.88	446,632.6	9.39

Table 10. Comparison of the metaheuristics SCA-Q-Learning.

		QL1			QL2			QL3			QL4			QL5		
Inst.	Opt.	Best	Avg	RPD	Best	Avg	RPD	Best	Avg	RPD	Best	Avg	RPD	Best	Avg	RPD
RW300-C	163,992.326	188,225.91	248,806.82	14.78	195,606.76	236,316.91	19.28	184,526.82	223,465.47	12.52	183,603.67	229,561.85	11.96	177,677.74	230,346.92	8.35
RW350-C	189,534.031	217,879.52	257,241.39	14.96	216,835.07	256,504.85	14.4	205,495.03	261,925.48	8.42	211,586.52	266,579.83	11.64	215,455.42	277,412.0	13.68
RW400-C	214,696.284	235,792.62	279,424.7	9.83	230,798.16	295,828.39	7.5	235,671.72	287,764.41	9.77	242,036.31	291,843.42	12.73	239,067.96	295,594.1	11.35
RW450-C	241,096.482	266,759.5	328,945.35	10.64	271,344.08	349,763.96	12.55	250,013.86	331,926.05	3.7	269,800.8	336,849.14	11.91	259,670.35	322,917.8	7.7
RW500-C	268,526.177	281,939.86	372,031.88	5.0	302,788.88	355,070.33	12.76	294,629.87	362,128.18	9.72	301,693.73	368,002.89	12.35	290,550.45	362,554.5	8.2
RW550-C	307,536.973	349,715.87	418,383.02	13.72	329,285.89	394,564.02	7.07	325,982.9	400,606.42	6.0	335,261.5	401,572.64	9.02	326,635.26	412,105.97	6.21
RW600-C	364,409.78	393,011.66	468,298.77	7.85	404,226.59	471,480.97	10.93	407,253.36	466,503.2	11.76	418,274.55	482,988.21	14.78	426,792.95	490,546.86	17.12
RW650-C	430,400.866	468,004.2	537,036.27	8.74	483,925.17	559,743.39	12.44	480,992.54	543,497.99	11.75	455,179.93	543,497.21	5.76	466,139.62	521,064.32	8.3
RW700-C	507,127.151	558,644.81	644,791.06	10.16	558,153.57	629,733.8	10.06	543,519.45	617,948.04	7.18	526,938.59	619,240.21	3.91	548,814.34	630,356.1	8.22
RW750-C	593,353.31	642,805.71	736,044.64	8.33	610,013.64	710,919.85	2.81	632,854.68	716,246.25	6.66	627,942.79	710,817.92	5.83	627,750.72	737,856.51	5.8
RW800-C	687,763.656	733,356.26	837,946.92	6.63	738,021.36	836,901.23	7.31	762,410.42	834,888.46	10.85	723,901.08	810,431.78	5.25	745,269.57	838,912.62	8.36
		394,194.17	466,268.26	10.06	394,636.29	463,347.97	10.65	393,031.88	458,809.09	8.94	390,565.41	460,125.92	9.56	393,074.94	465,424.34	9.39
RW300-E	612.204	632.53	787.52	3.32	627.73	850.08	2.54	662.77	824.1	8.26	685.78	810.94	12.02	690.43	829.65	12.78
RW350-E	708.081	775.24	966.1	9.48	729.99	916.66	3.09	771.07	935.3	8.9	758.6	935.43	7.13	779.8	942.15	10.13
RW400-E	802.088	881.25	1079.31	9.87	902.64	1064.21	12.54	858.14	1083.06	6.99	848.1	1088.94	5.74	880.95	1105.65	9.83
RW450-E	902.195	955.88	1163.21	5.95	981.23	1175.83	8.76	928.3	1220.16	2.89	1021.44	1176.07	13.22	1023.98	1192.25	13.5
RW500-E	1007.376	1115.7	1362.59	10.75	1133.5	1294.33	12.52	1066.27	1317.42	5.85	1114.7	1317.07	10.65	1071.88	1280.84	6.4
RW550-E	1122.621	1224.69	1492.48	9.09	1318.46	1495.19	17.44	1185.07	1505.19	5.56	1269.96	1512.38	13.12	1235.49	1520.3	10.05
RW600-E	1304.802	1451.05	1684.81	11.21	1440.04	1778.89	10.36	1409.39	1714.9	8.02	1461.23	1694.36	11.99	1477.48	1754.3	13.23
RW650-E	1545.005	1643.72	1958.12	6.39	1690.66	1941.53	9.43	1626.11	1969.11	5.25	1665.74	1963.95	7.81	1607.77	1972.57	4.06
RW700-E	1794.782	1947.43	2242.84	8.51	1960.46	2267.06	9.23	1929.02	2236.78	7.48	1895.92	2280.29	5.64	1878.92	2248.89	4.69
RW750-E	2099.338	2316.53	2580.85	10.35	2237.08	2591.88	6.56	2190.47	2579.14	4.34	2305.45	2623.37	9.82	2204.14	2579.3	4.99
RW800-E	2443.014	2654.95	2964.9	8.68	2783.78	3032.84	13.95	2572.41	2965.77	5.3	2607.03	3060.59	6.71	2557.59	2981.4	4.69
		1418.09	1662.07	8.51	1436.87	1673.5	9.67	1381.73	1668.27	6.26	1421.27	1678.49	9.44	1400.77	1673.39	8.58
RW300-C+E	164,604.53	178,117.75	218,093.56	8.21	174,480.66	218,954.42	6.0	178,552.1	228,386.25	8.47	175,423.38	227,357.91	6.57	177,436.63	217,508.53	7.8
RW350-C+E	190,242.112	211,036.84	265,385.47	10.93	202,716.35	254,733.66	6.56	225,144.99	278,282.7	18.35	208,876.32	263,848.8	9.79	208,058.71	255,324.14	9.37
RW400-C+E	215,498.372	233,635.68	300,872.86	8.42	252,481.47	302,436.59	17.16	232,996.34	305,644.45	8.12	246,074.32	313,417.21	14.19	232,666.38	302,175.97	7.97
RW450-C+E	241,998.678	252,589.42	342,970.47	4.38	273,417.79	334,499.99	12.98	269,754.56	340,325.28	11.47	270,090.54	328,724.7	11.61	255,095.97	333,278.29	5.41
RW500-C+E	269,533.553	312,593.43	361,128.9	15.98	300,549.66	372,079.4	11.51	282,690.22	379,290.8	4.88	285,100.9	368,225.15	5.78	301,263.97	370,004.36	11.77
RW550-C+E	308,696.291	321,599.14	401,669.81	4.18	335,613.38	414,082.42	8.72	346,142.33	410,142.05	12.13	344,482.35	413,813.22	11.59	353,362.3	410,923.12	14.47
RW600-C+E	365,784.894	380,615.59	472,031.82	4.05	413,513.62	483,327.05	13.05	406,735.23	478,947.71	11.2	413,275.63	491,019.25	12.98	400,832.43	475,439.54	9.58
RW650-C+E	432,031.377	462,077.04	537,604.78	6.95	460,609.49	541,804.88	6.61	466,736.14	542,475.14	8.03	465,974.21	528,471.46	7.86	463,620.51	552,228.91	7.31
RW700-C+E	508,928.933	546,000.95	637,165.32	7.28	549,446.46	616,198.15	7.96	541,173.79	640,621.23	6.34	559,246.37	639,752.38	9.89	561,079.68	636,865.36	10.25
RW750-C+E	595,461.955	642,054.47	728,172.58	7.82	647,973.23	714,062.88	8.82	663,569.76	732,790.77	11.44	627,776.99	729,641.43	5.43	674,321.71	745,833.69	13.24
RW800-C+E	690,374.634	735,470.14	832,503.27	6.53	730,552.55	820,013.4	5.82	746,408.39	861,105.24	8.12	742,962.6	847,258.14	7.62	768,856.17	852,352.07	11.37
		388,708.22	463,418.08	7.7	394,668.61	461,108.44	9.56	396,354.9	472,546.51	9.87	394,480.33	468,320.88	9.39	399,690.41	468,357.63	9.87

In order to analyze the GWO technique, which was the best-performing technique, it is necessary to quantify the RPD obtained in ranges. These categorizations were established according to a minimum and maximum range, average and standard deviation (Table 11).

Table 11. RPD distribution in GWO.

	Lower Limit	Upper Limit	Mean	Standard Deviation
S	0.93	16.74	7.68	3.15
V	3.22	29.28	12.84	4.81
QL	3.64	29.4	13.21	5.43
SARSA	0	27.39	12.59	5.38

With the ranges already established, the distribution in GWO of the different techniques is represented in Table 12.

Table 12. RPD distribution in GWO.

	[0, 7.5[	[7.5, 15[	[15, 22.5[	[22.5, +
S1	19	14	0	0
S2	20	12	1	0
S3	19	12	2	0
S4	16	16	1	0
V1	3	16	13	1
V2	4	23	4	2
V3	3	25	4	1
V4	6	16	10	1
QL1	5	13	14	1
QL2	8	14	8	3
QL3	4	19	5	5
QL4	3	19	10	1
QL5	4	20	8	1
SA1	7	19	7	0
SA2	10	14	8	1
SA3	4	16	12	1
SA4	2	20	10	1
SA5	3	18	8	4

Table 13 presents the parameters utilized in this research, providing information about the set of instances used. The table comprises several data columns, organized as follows:

1. **Inst.** lists each of the studied walls in sequential order.
2. **Opt.** displays the optimal value for each respective instance.
3. **Best** indicates the best value achieved during the execution.
4. **Shape** identifies the top-performing algorithm that reached the best value.
5. **Fitness** denotes the fitness or efficiency value of the best algorithm.
6. The remaining columns represent the design parameters.

This tabular representation effectively communicates the key parameters and findings from our research, allowing readers to quickly grasp the results and assess the performance of various algorithms in the study.

Table 13. Design parameters of the best results for each version.

Inst.	Opt.	Best	Shape	Concrete	Steel	Crowning	Base	Footing
RW300-C	163,992.326	172,736.65	QL4	25	2.8	0.17	0.35	0.45
RW350-C	189,534.031	201,487.94	S2	25	2.8	0.16	0.37	0.45
RW400-C	214,696.284	219,450.	S3	25	2.8	0.17	0.31	0.45
RW450-C	241,096.482	246,740.28	SA1	25	2.8	0.17	0.31	0.45
RW500-C	268,526.177	279,819.15	S3	25	2.8	0.15	0.31	0.47
RW550-C	307,536.973	322,283.21	S2	25	2.8	0.16	0.3	0.5
RW600-C	364,409.78	377,871.72	S3	25	4.2	0.17	0.3	0.54
RW650-C	430,400.866	451,496.13	V1	30	2.8	0.15	0.32	0.57
RW700-C	507,127.151	530,085.84	S3	25	2.8	0.24	0.34	0.65
RW750-C	593,353.31	611,414.67	SA2	30	2.8	0.18	0.35	0.67
RW800-C	687,763.656	710,899.7	SA3	30	2.8	0.16	0.39	0.74
RW300-E	612.204	631.33	S3	25	4.2	0.18	0.3	0.45
RW350-E	708.081	752.24	V2	25	2.8	0.15	0.38	0.45
RW400-E	802.088	849.79	S1	30	4.2	0.2	0.32	0.45
RW450-E	902.195	912.78	S3	25	2.8	0.15	0.31	0.45
RW500-E	1007.376	1036.58	S1	25	2.8	0.15	0.32	0.46
RW550-E	1122.621	1176.47	QL2	30	2.8	0.2	0.31	0.46
RW600-E	1304.802	1346.81	V2	30	2.8	0.16	0.32	0.5
RW650-E	1545.005	1588.32	S3	30	2.8	0.15	0.35	0.55
RW700-E	1794.782	1846.2	S4	30	2.8	0.16	0.35	0.6
RW750-E	2099.338	2175.81	QL2	40	2.8	0.16	0.3	0.59
RW800-E	2443.014	2491.57	S1	30	2.8	0.19	0.36	0.72
RW300-C+E	164,604.53	164,604.53	SA2	25	2.8	0.15	0.3	0.45
RW350-C+E	190,242.112	199,602.67	S1	25	2.8	0.15	0.3	0.49
RW400-C+E	215,498.372	223,604.65	SA2	25	2.8	0.15	0.3	0.48
RW450-C+E	241,998.678	256,669.92	SA1	25	2.8	0.15	0.3	0.49
RW500-C+E	269,533.553	282,150.29	S4	25	2.8	0.15	0.3	0.48
RW550-C+E	308,696.291	328,562.36	S3	25	2.8	0.2	0.35	0.47
RW600-C+E	365,784.894	381,018.45	SA5	25	2.8	0.17	0.32	0.54
RW650-C+E	432,031.377	459,287.25	V3	25	4.2	0.17	0.35	0.61
RW700-C+E	508,928.933	513,662.21	S4	25	2.8	0.17	0.33	0.65
RW750-C+E	595,461.955	619,227.4	S3	30	2.8	0.16	0.38	0.67
RW800-C+E	690,374.634	722,411.98	S1	30	4.2	0.21	0.4	0.72

5.1. Distribution Analysis

The violin plots (Figures 7–9) presented in this section offer a clear and concise visualization of the results obtained from our investigation of the algorithms employed. A representative instance was selected to showcase the results using the best-performing metaheuristic: GWO. Upon examining the plots, it is evident that the violins corresponding to Algorithms S1–S4 exhibit lower data dispersion compared to the others, signifying a greater efficiency in minimizing the problem. Overall, the violin plots provide an effective and lucid representation of the findings from our study, which will assist researchers and subject matter experts in making informed decisions when selecting techniques for future research and practical applications. The plots are structured as follows: the Y-axis displays the fitness range, which refers to the data density at that level, while the X-axis represents all the evaluated algorithms.

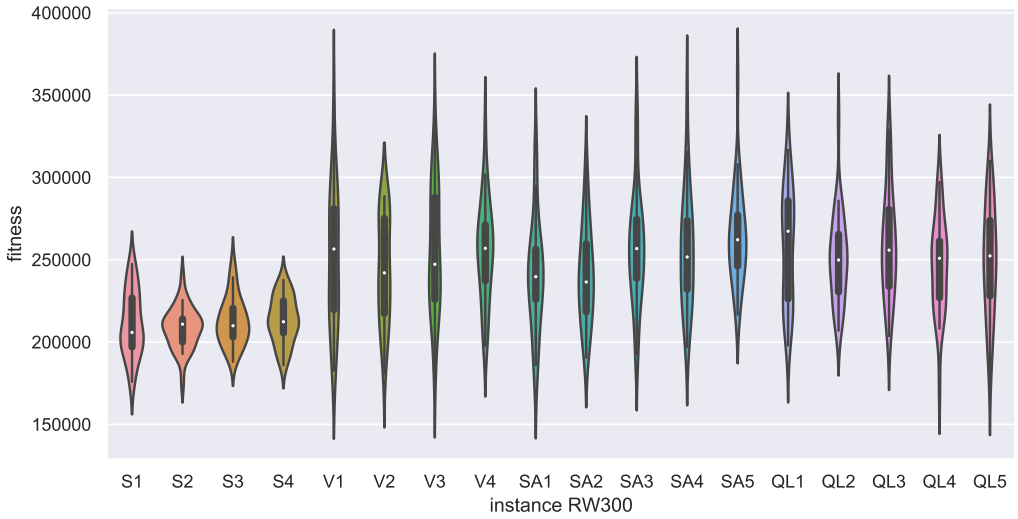

Figure 7. GWO Instance RW300—objective function cost.

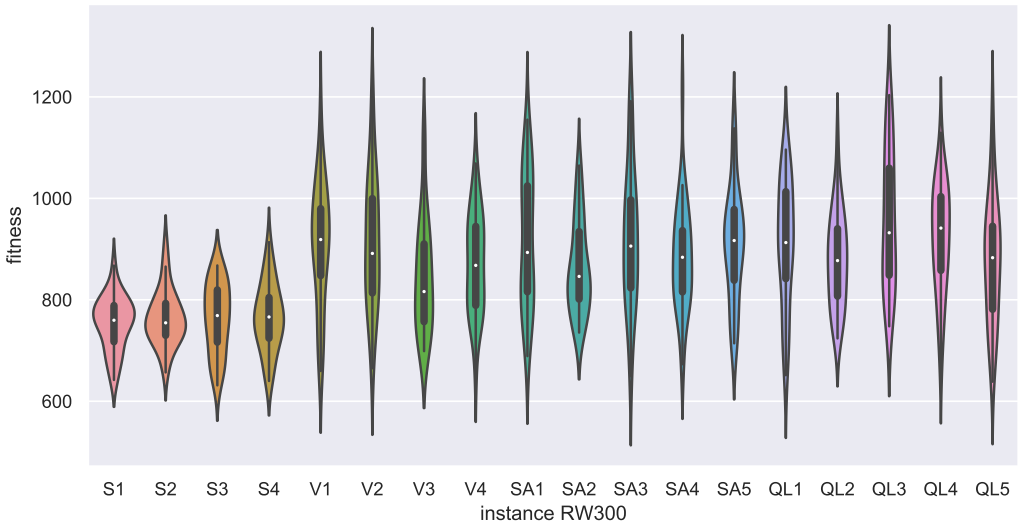

Figure 8. GWO Instance RW300—objective function CO_2 emissions.

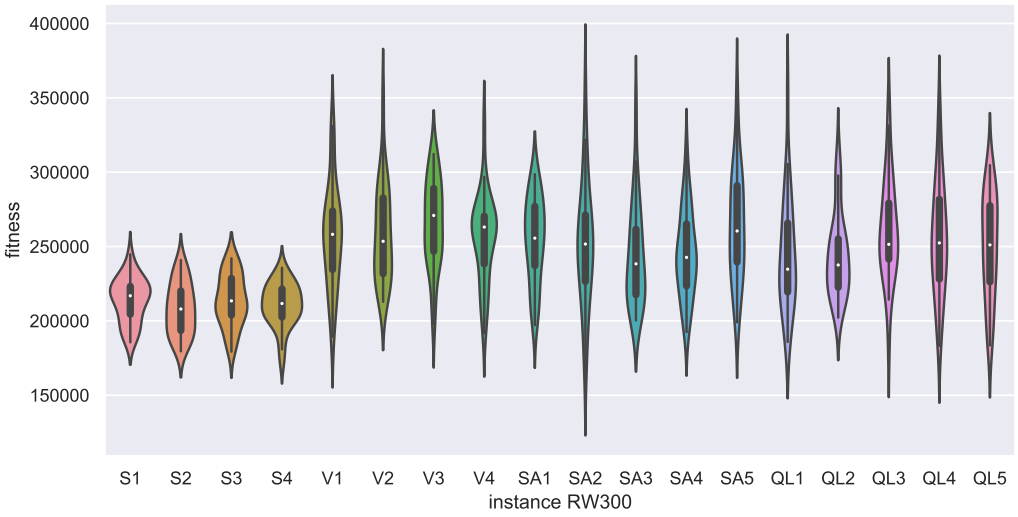

Figure 9. GWO Instance RW300—objective function cost + CO_2 emissions.

5.2. Statistical Test

The results displayed in Tables 14–16 concerning Algorithms S1–S4 in the Wilcoxon–Mann–Whitney statistical test corroborate earlier findings, suggesting that these algorithms excel in terms of minimization. Our statistical analysis reveals that the p-value of the test also supports these conclusions, as it is considerably lower than 0.05, signifying a statistically significant difference between the medians of algorithms S1–S4 and those of the remaining algorithms. In essence, the statistical test outcomes reinforce the violin plot findings, demonstrating that algorithms S1–S4 are indeed significantly superior.

The tables are structured as follows: the first row and column display the 18 algorithms under study and those to be compared. If the *p*-value is less than 0.05, the value is presented in bold and approximated to three decimal places. If the *p*-value exceeds 0.05, the value is replaced by ">0.05". When comparing identical algorithms, the symbol "-" is used to indicate that no comparison is made.

Table 14. Average *p*-value of GWO—objective function cost.

	S1	S2	S3	S4	V1	V2	V3	V4	SA1	SA2	SA3	SA4	SA5	QL1	QL2	QL3	QL4	QL5
S1	-	≥0.05	≥0.05	≥0.05	**0.00**	**0.00**	**0.00**	**0.00**	**0.00**	**0.00**	**0.00**	**0.00**	**0.00**	**0.00**	**0.00**	**0.00**	**0.00**	**0.00**
S2	≥0.05	-	≥0.05	≥0.05	**0.00**	**0.00**	**0.00**	**0.00**	**0.00**	**0.00**	**0.00**	**0.00**	**0.00**	**0.00**	**0.00**	**0.00**	**0.00**	**0.00**
S3	≥0.05	≥0.05	-	≥0.05	**0.00**	**0.00**	**0.00**	**0.00**	**0.00**	**0.00**	**0.00**	**0.00**	**0.00**	**0.00**	**0.00**	**0.00**	**0.00**	**0.00**
S4	≥0.05	≥0.05	≥0.05	-	**0.00**	**0.00**	**0.00**	**0.00**	**0.00**	**0.00**	**0.00**	**0.00**	**0.00**	**0.00**	**0.00**	**0.00**	**0.00**	**0.00**
V1	≥0.05	≥0.05	≥0.05	≥0.05	-	≥0.05	≥0.05	≥0.05	≥0.05	≥0.05	≥0.05	≥0.05	≥0.05	≥0.05	≥0.05	≥0.05	≥0.05	≥0.05
V2	≥0.05	≥0.05	≥0.05	≥0.05	≥0.05	-	≥0.05	≥0.05	≥0.05	≥0.05	≥0.05	≥0.05	≥0.05	≥0.05	≥0.05	≥0.05	≥0.05	≥0.05
V3	≥0.05	≥0.05	≥0.05	≥0.05	≥0.05	≥0.05	-	≥0.05	≥0.05	≥0.05	≥0.05	≥0.05	≥0.05	≥0.05	≥0.05	≥0.05	≥0.05	≥0.05
V4	≥0.05	≥0.05	≥0.05	≥0.05	≥0.05	≥0.05	≥0.05	-	≥0.05	≥0.05	≥0.05	≥0.05	≥0.05	≥0.05	≥0.05	≥0.05	≥0.05	≥0.05
SA1	≥0.05	≥0.05	≥0.05	≥0.05	≥0.05	≥0.05	≥0.05	≥0.05	-	≥0.05	≥0.05	≥0.05	≥0.05	≥0.05	≥0.05	≥0.05	≥0.05	≥0.05
SA2	≥0.05	≥0.05	≥0.05	≥0.05	≥0.05	≥0.05	≥0.05	≥0.05	≥0.05	-	≥0.05	≥0.05	≥0.05	≥0.05	≥0.05	≥0.05	≥0.05	≥0.05
SA3	≥0.05	≥0.05	≥0.05	≥0.05	≥0.05	≥0.05	≥0.05	≥0.05	≥0.05	≥0.05	-	≥0.05	≥0.05	≥0.05	≥0.05	≥0.05	≥0.05	≥0.05
SA4	≥0.05	≥0.05	≥0.05	≥0.05	≥0.05	≥0.05	≥0.05	≥0.05	≥0.05	≥0.05	≥0.05	-	≥0.05	≥0.05	≥0.05	≥0.05	≥0.05	≥0.05
SA5	≥0.05	≥0.05	≥0.05	≥0.05	≥0.05	≥0.05	≥0.05	≥0.05	≥0.05	≥0.05	≥0.05	≥0.05	-	≥0.05	≥0.05	≥0.05	≥0.05	≥0.05
QL1	≥0.05	≥0.05	≥0.05	≥0.05	≥0.05	≥0.05	≥0.05	≥0.05	≥0.05	≥0.05	≥0.05	≥0.05	≥0.05	-	≥0.05	≥0.05	≥0.05	≥0.05
QL2	≥0.05	≥0.05	≥0.05	≥0.05	≥0.05	≥0.05	≥0.05	≥0.05	≥0.05	≥0.05	≥0.05	≥0.05	≥0.05	≥0.05	-	≥0.05	≥0.05	≥0.05
QL3	≥0.05	≥0.05	≥0.05	≥0.05	≥0.05	≥0.05	≥0.05	≥0.05	≥0.05	≥0.05	≥0.05	≥0.05	≥0.05	≥0.05	≥0.05	-	≥0.05	≥0.05
QL4	≥0.05	≥0.05	≥0.05	≥0.05	≥0.05	≥0.05	≥0.05	≥0.05	≥0.05	≥0.05	≥0.05	≥0.05	≥0.05	≥0.05	≥0.05	≥0.05	-	≥0.05
QL5	≥0.05	≥0.05	≥0.05	≥0.05	≥0.05	≥0.05	≥0.05	≥0.05	≥0.05	≥0.05	≥0.05	≥0.05	≥0.05	≥0.05	≥0.05	≥0.05	≥0.05	-

Table 15. Average *p*-value of GWO—objective function CO_2 emissions.

	S1	S2	S3	S4	V1	V2	V3	V4	SA1	SA2	SA3	SA4	SA5	QL1	QL2	QL3	QL4	QL5
S1	-	≥0.05	≥0.05	≥0.05	**0.00**	**0.00**	**0.00**	**0.00**	**0.00**	**0.00**	**0.00**	**0.00**	**0.00**	**0.00**	**0.00**	**0.00**	**0.00**	**0.00**
S2	≥0.05	-	≥0.05	≥0.05	**0.00**	**0.00**	**0.00**	**0.00**	**0.00**	**0.00**	**0.00**	**0.00**	**0.00**	**0.00**	**0.00**	**0.00**	**0.00**	**0.00**
S3	≥0.05	≥0.05	-	≥0.05	**0.00**	**0.00**	**0.00**	**0.00**	**0.00**	**0.00**	**0.00**	**0.00**	**0.00**	**0.00**	**0.00**	**0.00**	**0.00**	**0.00**
S4	≥0.05	≥0.05	≥0.05	-	**0.00**	**0.00**	**0.00**	**0.00**	**0.00**	**0.00**	**0.00**	**0.00**	**0.00**	**0.00**	**0.00**	**0.00**	**0.00**	**0.00**
V1	≥0.05	≥0.05	≥0.05	≥0.05	-	≥0.05	≥0.05	≥0.05	≥0.05	≥0.05	≥0.05	≥0.05	≥0.05	≥0.05	≥0.05	≥0.05	≥0.05	≥0.05
V2	≥0.05	≥0.05	≥0.05	≥0.05	≥0.05	-	≥0.05	≥0.05	≥0.05	≥0.05	≥0.05	≥0.05	≥0.05	≥0.05	≥0.05	≥0.05	≥0.05	≥0.05
V3	≥0.05	≥0.05	≥0.05	≥0.05	≥0.05	≥0.05	-	≥0.05	≥0.05	≥0.05	≥0.05	≥0.05	≥0.05	≥0.05	≥0.05	≥0.05	≥0.05	≥0.05
V4	≥0.05	≥0.05	≥0.05	≥0.05	≥0.05	≥0.05	≥0.05	-	≥0.05	≥0.05	≥0.05	≥0.05	≥0.05	≥0.05	≥0.05	≥0.05	≥0.05	≥0.05
SA1	≥0.05	≥0.05	≥0.05	≥0.05	≥0.05	≥0.05	≥0.05	≥0.05	-	≥0.05	≥0.05	≥0.05	≥0.05	≥0.05	≥0.05	≥0.05	≥0.05	≥0.05
SA2	≥0.05	≥0.05	≥0.05	≥0.05	≥0.05	≥0.05	≥0.05	≥0.05	≥0.05	-	≥0.05	≥0.05	≥0.05	≥0.05	≥0.05	≥0.05	≥0.05	≥0.05
SA3	≥0.05	≥0.05	≥0.05	≥0.05	≥0.05	≥0.05	≥0.05	≥0.05	≥0.05	≥0.05	-	≥0.05	≥0.05	≥0.05	≥0.05	≥0.05	≥0.05	≥0.05
SA4	≥0.05	≥0.05	≥0.05	≥0.05	≥0.05	≥0.05	≥0.05	≥0.05	≥0.05	≥0.05	≥0.05	-	≥0.05	≥0.05	≥0.05	≥0.05	≥0.05	≥0.05
SA5	≥0.05	≥0.05	≥0.05	≥0.05	≥0.05	≥0.05	≥0.05	≥0.05	≥0.05	≥0.05	≥0.05	≥0.05	-	≥0.05	≥0.05	≥0.05	≥0.05	≥0.05
QL1	≥0.05	≥0.05	≥0.05	≥0.05	≥0.05	≥0.05	≥0.05	≥0.05	≥0.05	≥0.05	≥0.05	≥0.05	≥0.05	-	≥0.05	≥0.05	≥0.05	≥0.05
QL2	≥0.05	≥0.05	≥0.05	≥0.05	≥0.05	≥0.05	≥0.05	≥0.05	≥0.05	≥0.05	≥0.05	≥0.05	≥0.05	≥0.05	-	≥0.05	≥0.05	≥0.05
QL3	≥0.05	≥0.05	≥0.05	≥0.05	≥0.05	≥0.05	≥0.05	≥0.05	≥0.05	≥0.05	≥0.05	≥0.05	≥0.05	≥0.05	≥0.05	-	≥0.05	≥0.05
QL4	≥0.05	≥0.05	≥0.05	≥0.05	≥0.05	≥0.05	≥0.05	≥0.05	≥0.05	≥0.05	≥0.05	≥0.05	≥0.05	≥0.05	≥0.05	≥0.05	-	≥0.05
QL5	≥0.05	≥0.05	≥0.05	≥0.05	≥0.05	≥0.05	≥0.05	≥0.05	≥0.05	≥0.05	≥0.05	≥0.05	≥0.05	≥0.05	≥0.05	≥0.05	≥0.05	-

Table 16. Average *p*-value of GWO—objective function cost + CO_2 emissions.

	S1	S2	S3	S4	V1	V2	V3	V4	SA1	SA2	SA3	SA4	SA5	QL1	QL2	QL3	QL4	QL5
S1	-	≥0.05	≥0.05	≥0.05	**0.00**	**0.00**	**0.00**	**0.00**	**0.00**	**0.00**	**0.00**	**0.00**	**0.00**	**0.00**	**0.00**	**0.00**	**0.00**	**0.00**
S2	≥0.05	-	≥0.05	≥0.05	**0.00**	**0.00**	**0.00**	**0.00**	**0.00**	**0.00**	**0.00**	**0.00**	**0.00**	**0.00**	**0.00**	**0.00**	**0.00**	**0.00**
S3	≥0.05	≥0.05	-	≥0.05	**0.00**	**0.00**	**0.00**	**0.00**	**0.00**	**0.00**	**0.00**	**0.00**	**0.00**	**0.00**	**0.00**	**0.00**	**0.00**	**0.00**
S4	≥0.05	≥0.05	≥0.05	-	**0.00**	**0.00**	**0.00**	**0.00**	**0.00**	**0.00**	**0.00**	**0.00**	**0.00**	**0.00**	**0.00**	**0.00**	**0.00**	**0.00**
V1	≥0.05	≥0.05	≥0.05	≥0.05	-	≥0.05	≥0.05	≥0.05	≥0.05	≥0.05	≥0.05	≥0.05	≥0.05	≥0.05	≥0.05	≥0.05	≥0.05	≥0.05
V2	≥0.05	≥0.05	≥0.05	≥0.05	≥0.05	-	≥0.05	≥0.05	≥0.05	≥0.05	≥0.05	≥0.05	≥0.05	≥0.05	≥0.05	≥0.05	≥0.05	≥0.05
V3	≥0.05	≥0.05	≥0.05	≥0.05	≥0.05	≥0.05	-	≥0.05	≥0.05	≥0.05	≥0.05	≥0.05	≥0.05	≥0.05	≥0.05	≥0.05	≥0.05	≥0.05
V4	≥0.05	≥0.05	≥0.05	≥0.05	≥0.05	≥0.05	≥0.05	-	≥0.05	≥0.05	≥0.05	≥0.05	≥0.05	≥0.05	≥0.05	≥0.05	≥0.05	≥0.05
SA1	≥0.05	≥0.05	≥0.05	≥0.05	≥0.05	≥0.05	≥0.05	≥0.05	-	≥0.05	≥0.05	≥0.05	≥0.05	≥0.05	≥0.05	≥0.05	≥0.05	≥0.05

Table 16. *Cont.*

	S1	S2	S3	S4	V1	V2	V3	V4	SA1	SA2	SA3	SA4	SA5	QL1	QL2	QL3	QL4	QL5
SA2	≥0.05	≥0.05	≥0.05	≥0.05	≥0.05	≥0.05	≥0.05	≥0.05	≥0.05	-	≥0.05	≥0.05	≥0.05	≥0.05	≥0.05	≥0.05	≥0.05	≥0.05
SA3	≥0.05	≥0.05	≥0.05	≥0.05	≥0.05	≥0.05	≥0.05	≥0.05	≥0.05	≥0.05	-	≥0.05	≥0.05	≥0.05	≥0.05	≥0.05	≥0.05	≥0.05
SA4	≥0.05	≥0.05	≥0.05	≥0.05	≥0.05	≥0.05	≥0.05	≥0.05	≥0.05	≥0.05	≥0.05	-	≥0.05	≥0.05	≥0.05	≥0.05	≥0.05	≥0.05
SA5	≥0.05	≥0.05	≥0.05	≥0.05	≥0.05	≥0.05	≥0.05	≥0.05	≥0.05	≥0.05	≥0.05	≥0.05	-	≥0.05	≥0.05	≥0.05	≥0.05	≥0.05
QL1	≥0.05	≥0.05	≥0.05	≥0.05	≥0.05	≥0.05	≥0.05	≥0.05	≥0.05	≥0.05	≥0.05	≥0.05	≥0.05	-	≥0.05	≥0.05	≥0.05	≥0.05
QL2	≥0.05	≥0.05	≥0.05	≥0.05	≥0.05	≥0.05	≥0.05	≥0.05	≥0.05	≥0.05	≥0.05	≥0.05	≥0.05	≥0.05	-	≥0.05	≥0.05	≥0.05
QL3	≥0.05	≥0.05	≥0.05	≥0.05	≥0.05	≥0.05	≥0.05	≥0.05	≥0.05	≥0.05	≥0.05	≥0.05	≥0.05	≥0.05	≥0.05	-	≥0.05	≥0.05
QL4	≥0.05	≥0.05	≥0.05	≥0.05	≥0.05	≥0.05	≥0.05	≥0.05	≥0.05	≥0.05	≥0.05	≥0.05	≥0.05	≥0.05	≥0.05	≥0.05	-	≥0.05
QL5	≥0.05	≥0.05	≥0.05	≥0.05	≥0.05	≥0.05	≥0.05	≥0.05	≥0.05	≥0.05	≥0.05	≥0.05	≥0.05	≥0.05	≥0.05	≥0.05	≥0.05	-

6. Conclusions

This paper introduces a novel approach to optimizing retaining structural wall designs by implementing an innovative discretization method that utilizes reinforcement learning and transfer functions. Conventional structural design practices rely on empirical knowledge and experience, resulting in designs that prioritize strength, operability, and durability. However, these designs have room for improvement by minimizing their associated costs and CO_2 emissions.

Designs created using experience and empirical knowledge can produce feasible results that are often acceptable in cost and operability. However, these designs do not necessarily represent the optimal solution for a given scenario. Retaining wall design problems are considered combinatorial optimization challenges, which can quickly result in a combinatorial explosion due to the large number of variables and extensive discrete domains involved. Consequently, it is crucial to use incomplete techniques to solve these problems within a reasonable computational time frame. Metaheuristics have emerged as a prominent solution for addressing such challenges.

This work outlines the calculation procedure for determining the dimensions of a retaining wall, framing it as an optimization problem. Three metaheuristic techniques are implemented to evaluate their performance and use various transfer functions for the discretization process. Additionally, a novel discretization method, based on Q-Learning and SARSA, is employed to select the appropriate transfer function for each iteration during the discretization process.

The proposed model aims to minimize costs, CO_2 emissions, or a weighted combination of both, considering the design parameters detailed in Table 1 as problem variables, with the constraints being those inherent to the design of a retaining wall, as detailed in Section 2.1. Experimental results have been obtained using the Sine Cosine Algorithm (SCA), Whale Optimization Algorithm (WOA), and Gray Wolf Optimization (GWO) metaheuristics, with each run independently for 31 runs across 11 problem instances. After evaluating all the techniques across the three objective functions, the *p*-values obtained by the Wilcoxon–Mann–Whitney test for the GWO are presented, revealing the best results for the static versions using S-shaped transfer functions. GWO demonstrated significant differences in its results, indicating that it outperformed the other techniques for this specific problem. This does not imply that the other techniques are inadequate; rather, it suggests that the GWO S-shaped technique performs better for this particular problem.

The development of new optimization techniques, such as the one in this article, is crucial. It not only benefits the engineering profession, but also has considerable environmental and economic implications. By optimizing design processes and reducing costs and CO_2 emissions, the industry can contribute to a more sustainable future. One discussion point in this work is selecting transfer functions used in the discretization process. S-shaped functions provided the best results in terms of minimizing costs and CO_2 emissions, as demonstrated. However, other functions might offer better results for different problems or under various conditions, which the non-free lunch theorem also supports. Investigating how different transfer functions could affect results and determining an optimal function for a specific problem would be interesting.

Another discussion is the comparison of the results obtained with the different metaheuristic algorithms used in this work. While GWO with S-shaped transfer gave the best results, the other two algorithms also produced acceptable results. However, it could be argued that more metaheuristic algorithms should be compared to fully evaluate the effectiveness of this technique in retaining wall design optimization. In addition, it would be interesting to compare the results obtained with the approach proposed in this work with other retaining wall design optimization approaches, such as those based on other machine learning techniques.

Finally, the application of this approach to real-world design problems could be discussed. While the results are promising, it is possible that the implementation of this approach in real construction projects may be more complicated than the experimental results suggest. For example, there may be time and resource constraints that were not accounted for in this work that could affect the ability to use this approach in a real construction environment. Therefore, it could be argued that further research is needed to determine how this approach can be effectively implemented in real-world construction projects and how the practical challenges associated with its implementation can be addressed.

Future research should consider a broader range of assessment techniques, parameter variations, and other considerations. These distinctions could lead to results that are closer to reality. There also remains the challenge of extending these techniques to other construction problems, allowing specific processes to be designed more efficiently and accurately. Overall, the paper presents a promising approach to improving civil work designs, and the results suggest that further research in this field could lead to significant advances in the field.

Author Contributions: J.L.-R.: Writing—original draft, data curation, investigation, validation, software, visualization, formal analysis. D.O.: Investigation, methodology, project administration, resources, writing—original draft. R.S.: Investigation, methodology, project administration, resources, writing—original draft. N.C.-A.: Writing—original draft, visualization, formal analysis. V.Y.: Writing—review and editing. J.G.: Supervision, conceptualization, funding acquisition, investigation, methodology, writing—review and editing, project administration, resources, formal analysis. All authors have read and agreed to the published version of the manuscript.

Funding: Víctor Yepes is supported by Grant PID2020-117056RB-I00 funded by MCIN/AEI/10.13039/501100011033 and by "ERDF A way of making Europe". José Lemus-Romani is supported by National Agency for Research and Development (ANID)/Scholarship Program/DOCTORADO NACIONAL/2019-21191692.

Data Availability Statement: https://github.com/joselemusr/DSS-Retaining-walls.

Conflicts of Interest: The authors declare no conflict of interest.

Abbreviations

The following abbreviations are used in this manuscript:

Acronyms Part 1	
MH	Metaheuristics
FEM	Finite Element Model
SCA	Sine-Cosine Algorithm
WOA	Whale Optimization Algorithm
GWO	Gray Wolf Optimization
MINLP	Mixed-Integer Non-Linear Programming
qe	Static thrust exerted by the fill [T/m]
γ	Existing soil density [T/m^3].
z	Height of the wall [m].
c	Static thrust coefficient.
b	Wall width, corresponding to 1 [m].
qs	Seismic thrust exerted by the backfill [T/m].

$gamma$	Existing soil density [T/m^3].
hz	Height of wall [m].
cs	Seismic thrust coefficient.
MsA	Moment calculated at point A [T · m].
M_{active}	Static moment generated by the ground at point A [T · m].
$M_{seismic}$	Seismic moment generated by the ground at point A [T · m].
M_{pp}	Moment generated by the self-weight at point A [T · m].
$d1$	Distance from the centroid of the prismatic section of the wall to point A [m].
$N1$	Eigenweight of the prismatic section of the wall [T].
$d2$	Distance from the centroid of the triangular section of the wall to point A [m].
$N2$	Eigenweight of the triangular section of the wall [T].
MA	Total moment at point A [T · m].
MsA	Moment calculated at point A [T · m].
M_{pp}	Moment generated by self-weight at point A [T · m].
Meu	Design moment [T · m].
γf	Moment majorization factor.
Nu	Design axial load [T].
Nt	Own weight of the wall [T].
μ	Dimensionless calculation factor.
ϕ	Reduction factor for flexocompression equal to 0.83.
β	Reduction of the characteristic strength of concrete equal to 0.85.
$f'c$	Characteristic resistance of concrete to compression [T/m^2].
b	Width of the wall, corresponding to 1 [m].
d	Width of the base of the wall without covering [m].
v	Dimensionless shear factor in the structure.
w	Calculation ratio for the steel area.
A	Dimensionless calculation factor.
f_y	Width of the base of the wall without covering [m].
M_r	Overturning resisting moment [T · m].
Ns	Self-weight of soil on bottom [T].
$x1$	Distance from the centroid of Ns to point B [m].
Nm	Dead weight of the wall wedge and the soil above it [T].
$x2$	Distance from the centroid of Nm to point B [m].
$N1$	Self weight of the prismatic section of the wall [T].
$x3$	Distance from the centroid of N1 to point B [m].
Nf	Self weight of the wall foundation [T].
$x4$	Distance from the centroid of Nf to point B [m].
MSB	Moment resisting overturning [T].
$M_{active}B$	Self-weight of the soil on the bottom [T].
$M_{seismic}B$	Distance from the centroid of Ns to point B [m].
$FSSV$	Overturning seismic safety factor.
$FSEV$	Rollover static safety factor.
$Fsol$	Slip requesting force [T].
$Fres$	Slip resistant forces [T].
$FSSD$	Seismic slip safety factor.
L	Total length of foundation [m].
g	Section of the foundation supported on the ground [m].
e	Eccentricity of forces [m].
Acronyms Part 2	
$\sigma_effective$	Effective stress applied to the foundation soil.
$Mdesign$	Design moment of reinforcement reinforcement [T · m].
Mdl	Design moment of longitudinal reinforcement [T · m].
Bdt	Maximum foundation flight [m].
Bm	Width of wall base [m].
Pp	Self-weight of the wall [T].
Mdt	Design moment of transverse reinforcement [T · m].
T	Design stress [T].
Md	Corresponding design moment (Mdl or Mdt) [T · m].

d'	Effective shoe height (height without cover) [m].
As	Required steel area [cm^2].
Fy	Yield stress of steel [T/cm^2].
$emin$	Minimum amount of steel required [cm^2].
Ag	Longitudinal or cross-sectional area of the footing, as appropriate [cm^2].
Vu	Design cut request [T].
Vc	Shear strength of concrete section [T].
λ	Concrete modification factor. For normal concrete, $\lambda = 1$.
μlim	Calculation limit dimensionless factor, equal to 0.3047 for the case of analysis.
CMt	Total cost of retaining wall [CLP].
$CM1$	Cost of one cubic meter of concrete [CLP/m^3].
$PM1$	Total volume of concrete used [m^3].
$CM2$	Cost of one kilogram of steel [CLP/kg].
$PM2$	Total kilograms of steel used [kg].
EMt	Total carbon dioxide emissions [T].
$EM1$	Tons of carbon emitted per cubic meter of concrete [T/m^3].
$PM1$	Total volume of concrete used [m^3].
$EM2$	Tons of carbon emitted per kilogram of steel [T/kg].
$PM2$	Total kilograms of steel used [kg].
$CEMt$	Total between the sum of cost and emissions.
BSS	Binarization Schemes Selector
QL	Q-Learning
$\bar{x}^d$	Average of individuals in dimension d
x_i^d	Value of the i-th individual in dimension d
n	Number of individuals in the population
l	Size of the dimension of the individuals
Div	Determination of the diversity state
Div_{max}	Maximum value of the diversity state found
MH	Metahuristics
RPD	Relative Percentage Deviation

References

1. Mergos, P.E.; Mantoglou, F. Optimum design of reinforced concrete retaining walls with the flower pollination algorithm. *Struct. Multidiscip. Optim.* **2020**, *61*, 575–585. [CrossRef]
2. Choi, J.H. Strategy for reducing carbon dioxide emissions from maintenance and rehabilitation of highway pavement. *J. Clean. Prod.* **2019**, *209*, 88–100. [CrossRef]
3. Barandica, J.M.; Fernández-Sánchez, G.; Berzosa, Á.; Delgado, J.A.; Acosta, F.J. Applying life cycle thinking to reduce greenhouse gas emissions from road projects. *J. Clean. Prod.* **2013**, *57*, 79–91. [CrossRef]
4. Lee, K.H.; Kim, H.J.; Kwon, S.H.; Kim, M.J. The program development for environmental quality level and evaluation of carbon dioxide emission in construction works. *LHI J. Land Hous. Urban Aff.* **2012**, *3*, 399–406. [CrossRef]
5. Pons, J.J.; Penadés-Plà, V.; Yepes, V.; Martí, J.V. Life cycle assessment of earth-retaining walls: An environmental comparison. *J. Clean. Prod.* **2018**, *192*, 411–420. [CrossRef]
6. Eleftheriadis, S.; Duffour, P.; Greening, P.; James, J.; Stephenson, B.; Mumovic, D. Investigating relationships between cost and CO_2 emissions in reinforced concrete structures using a BIM-based design optimisation approach. *Energy Build.* **2018**, *166*, 330–346. [CrossRef]
7. Jelušič, P.; Žlender, B. Optimal design of pad footing based on MINLP optimization. *Soils Found.* **2018**, *58*, 277–289. [CrossRef]
8. Chen, J.; Cho, Y.K. CrackEmbed: Point feature embedding for crack segmentation from disaster site point clouds with anomaly detection. *Adv. Eng. Inform.* **2022**, *52*, 101550. [CrossRef]
9. Zhou, Q.; Qu, Z.; Wang, S.Y.; Bao, K.H. A Method of Potentially Promising Network for Crack Detection With Enhanced Convolution and Dynamic Feature Fusion. *IEEE Trans. Intell. Transp. Syst.* **2022**, *23*, 18736–18745. [CrossRef]
10. Wang, W.; Su, C. Automatic Classification of Reinforced Concrete Bridge Defects Using the Hybrid Network. *Arab. J. Sci. Eng.* **2022**, *47*, 5187–5197. [CrossRef]
11. Duan, R.; Deng, H.; Tian, M.; Deng, Y.; Lin, J. SODA: Site Object Detection dAtaset for Deep Learning in Construction. *arXiv* **2022**, arXiv:2202.09554.
12. Greeshma, A.; Edayadiyil, J.B. Automated progress monitoring of construction projects using Machine learning and image processing approach. *Mater. Today Proc.* **2022**, *65*, 554–563.
13. Sharma, S.; Saha, A.K.; Lohar, G. Optimization of weight and cost of cantilever retaining wall by a hybrid metaheuristic algorithm. *Eng. Comput.* **2022**, *38*, 2897–2923. [CrossRef]

14. García, J.; Yepes, V.; Martí, J.V. A hybrid k-means cuckoo search algorithm applied to the counterfort retaining walls problem. *Mathematics* **2020**, *8*, 555. [CrossRef]
15. Kaveh, A.; Biabani Hamedani, K.; Zaerreza, A. A set theoretical shuffled shepherd optimization algorithm for optimal design of cantilever retaining wall structures. *Eng. Comput.* **2021**, *37*, 3265–3282. [CrossRef]
16. Mann, H.B.; Whitney, D.R. On a test of whether one of two random variables is stochastically larger than the other. *Ann. Math. Stat.* **1947**, *18*, 50–60. [CrossRef]
17. Belarbi, A. *ACI 318-14. Building Code Requirements for Structural Concrete*; American Concrete Institute: Farmington Hills, MI, USA, 2014.
18. de Carreteras, M. *Manual de Carreteras*; Ministerio de Obras Publicas, Dirección de Vialidad: Santiago, Chile , 2015; Volume 3. Instrucciones y criterios de diseño.
19. Díaz López, E.; Martínez Prieto, A.; Gálvez Lio, D. Una implementación de la meta-heuristica "Optimización en Mallas Variables" en la arquitectura CUDA. *Rev. Cuba. Cienc. Inform.* **2016**, *10*, 42–56.
20. Blum, C.; Roli, A. Metaheuristics in combinatorial optimization: Overview and conceptual comparison. *ACM Comput. Surv. (CSUR)* **2003**, *35*, 268–308. [CrossRef]
21. Talbi, E.G. *Metaheuristics: From Design to Implementation*; John Wiley & Sons: Hoboken, NJ, USA, 2009; Volume 74.
22. Mirjalili, S.; Lewis, A. The whale optimization algorithm. *Adv. Eng. Softw.* **2016**, *95*, 51–67. [CrossRef]
23. Mirjalili, S. SCA: A sine cosine algorithm for solving optimization problems. *Knowl.-Based Syst.* **2016**, *96*, 120–133. [CrossRef]
24. Mirjalili, S.; Mirjalili, S.M.; Lewis, A. Grey wolf optimizer. *Adv. Eng. Softw.* **2014**, *69*, 46–61. [CrossRef]
25. Crawford, B.; Soto, R.; Lemus-Romani, J.; Becerra-Rozas, M.; Lanza-Gutiérrez, J.M.; Caballé, N.; Castillo, M.; Tapia, D.; Cisternas-Caneo, F.; García, J.; et al. Q-learnheuristics: Towards data-driven balanced metaheuristics. *Mathematics* **2021**, *9*, 1839. [CrossRef]
26. Lemus-Romani, J.; Becerra-Rozas, M.; Crawford, B.; Soto, R.; Cisternas-Caneo, F.; Vega, E.; Castillo, M.; Tapia, D.; Astorga, G.; Palma, W.; et al. A novel learning-based binarization scheme selector for swarm algorithms solving combinatorial problems. *Mathematics* **2021**, *9*, 2887. [CrossRef]
27. Becerra-Rozas, M.; Lemus-Romani, J.; Cisternas-Caneo, F.; Crawford, B.; Soto, R.; García, J. Swarm-Inspired Computing to Solve Binary Optimization Problems: A Backward Q-Learning Binarization Scheme Selector. *Mathematics* **2022**, *10*, 4776. [CrossRef]
28. Becerra-Rozas, M.; Cisternas-Caneo, F.; Crawford, B.; Soto, R.; García, J.; Astorga, G.; Palma, W. Embedded Learning Approaches in the Whale Optimizer to Solve Coverage Combinatorial Problems. *Mathematics* **2022**, *10*, 4529. [CrossRef]
29. Watkins, C.J.; Dayan, P. Q-learning. *Mach. Learn.* **1992**, *8*, 279–292. [CrossRef]
30. Sutton, R.S.; Barto, A.G. *Reinforcement Learning: An Introduction*; MIT Press: Cambridge, MA, USA, 2018.
31. Xu, Y.; Pi, D. A reinforcement learning-based communication topology in particle swarm optimization. *Neural Comput. Appl.* **2019**, 32, 10007–10032. [CrossRef]
32. Nareyek, A. Choosing search heuristics by non-stationary reinforcement learning. In *Metaheuristics: Computer Decision-Making*; Springer: Berlin/Heidelberg, Germany, 2003; pp. 523–544.
33. Salleh, M.N.M.; Hussain, K.; Cheng, S.; Shi, Y.; Muhammad, A.; Ullah, G.; Naseem, R. Exploration and exploitation measurement in swarm-based metaheuristic algorithms: An empirical analysis. In Proceedings of the International Conference on Soft Computing and Data Mining, Johor, Malaysia, 6–8 February 2018; Springer: Berlin/Heidelberg, Germany, 2018; pp. 24–32.
34. Cheng, S.; Shi, Y.; Qin, Q.; Zhang, Q.; Bai, R. Population Diversity Maintenance In Brain Storm Optimization Algorithm. *J. Artif. Intell. Soft Comput. Res.* **2014**, *4*, 83–97. [CrossRef]
35. Hussain, K.; Zhu, W.; Salleh, M.N.M. Long-term memory Harris' hawk optimization for high dimensional and optimal power flow problems. *IEEE Access* **2019**, *7*, 147596–147616. [CrossRef]
36. Morales-Castañeda, B.; Zaldivar, D.; Cuevas, E.; Fausto, F.; Rodríguez, A. A better balance in metaheuristic algorithms: Does it exist? *Swarm Evol. Comput.* **2020**, *54*, 100671. [CrossRef]
37. Crawford, B.; Soto, R.; Astorga, G.; García, J.; Castro, C.; Paredes, F. Putting continuous metaheuristics to work in binary search spaces. *Complexity* **2017**, *2017*, 8404231. [CrossRef]
38. Becerra-Rozas, M.; Lemus-Romani, J.; Cisternas-Caneo, F.; Crawford, B.; Soto, R.; Astorga, G.; Castro, C.; García, J. Continuous Metaheuristics for Binary Optimization Problems: An Updated Systematic Literature Review. *Mathematics* **2022**, *11*, 129. [CrossRef]